

ADVANCED SOLID ELECTROLYTE CELL FOR CO₂ AND H₂O ELECTROLYSIS

(NASA-CR-152093) ADVANCED SOLID ELECTROLYTE
CELL FOR CO₂ AND H₂O ELECTROLYSIS Final
Report (Life Systems, Inc., Cleveland,
Ohio.) 52 p HC A04/MF A01 CSCL 07D

N78-21235

Unclas
G3/25 14979

FINAL REPORT

by

J.W. Shumar and T.A. Berger

March, 1978

Prepared Under Contract NAS2-7862

by

Life Systems, Inc.

Cleveland, OH 44122

for

AMES RESEARCH CENTER
National Aeronautics and Space Administration



ER-190-25

ADVANCED SOLID ELECTROLYTE CELL
FOR CO₂ AND H₂O ELECTROLYSIS

FINAL REPORT

by

J. W. Shumar and T. A. Berger

March, 1978

Distribution of this report is provided in the interest of information exchange. Responsibility for the contents resides in the authors or organization that prepared it.

Prepared Under Contract NAS2-7862

by

Life Systems, Inc.
Cleveland, OH 44122

for

Ames Research Center
National Aeronautics and Space Administration

FOREWORD

The development work described in this report was performed by Life Systems, Inc. under NASA Contract NAS2-7862. The work was performed during the period beginning April 1, 1976 through March 31, 1978. The Program Manager was J. W. Shumar. Technical support was provided by J. David Powell in Electrical Engineering, Terry A. Berger in Electrochemistry and Franz H. Schubert in Mechanical Engineering.

The Contract's Technical Monitor was P. D. Quattrone, Chief, Advanced Life Support Project Office, NASA Ames Research Center, Moffett Field, CA.

TABLE OF CONTENTS

	<u>PAGE</u>
LIST OF FIGURES	11
LIST OF TABLES	111
ACRONYMS	111
SUMMARY	1
INTRODUCTION	2
ELECTROLYZER TUBE CELL	4
Electrolyzer Tube Cell Function and Reactions	4
Electrolyzer Tube Cell Design Characteristics	4
Electrolyzer Tube Cell Description	10
TEST SUPPORT ACCESSORIES	13
Single Cell Test Stand	13
Electrolyzer Tube Cell Leak Test Apparatus	18
PROGRAM TESTING	18
Electrolyzer Tube Cell Checkout Tests	18
Leak Tests	18
Zirconium Oxide Breakdown Voltage	18
CO ₂ Electrolysis Current Density Spans	20
Wafer Electrolysis Current Density Spans	23
Parametric Testing	23
Effect of Operating Temperature	23
Effect of Backpressure	23
Effect of Feed Gas Flow Rate	27
Effect of Feed Gas Composition on Performance	27
Endurance Tests	27
SUPPORTING TECHNOLOGY STUDIES	38
Ceramic Cement Seal Development	38
Commercial Electroding Technique	42
TUBE CELL TERMINAL VOLTAGE IMPROVEMENT STUDY	42
CONCLUSIONS	42
RECOMMENDATIONS	44
REFERENCES	46

LIST OF FIGURES

<u>FIGURE</u>		<u>PAGE</u>
1	Descriptive Schematic of CO ₂ and Water Electrolysis Reactions	5
2	Electrolyzer Tube Cell Seals	8
3	Electrolyzer Drum Depicting Number and Type of Seals	9
4	Electrolyzer Tube Cell Assembly	11
5	Ceramic Inlet Tube Subassembly as Positioned in Electrolyte Tube	12
6	Three-Position Single Cell Test Stand Schematic	14
7	Single Cell Test Stand, Front View	16
8	Single Cell Test Stand, Rear View	17
9	Leak Test Apparatus Schematic	19
10	Yttria Stabilized Zirconium Oxide Breakdown Voltage	21
11	Typical Current Density Span, CO ₂ Electrolysis	22
12	Current Density Span, Water Electrolysis	24
13	Cell Voltage Versus Operating Temperature	25
14	Oxygen Purity Versus Differential Pressure	26
15	CO ₂ Electrolysis Current Density Spans at Various CO ₂ Flows	29
16	Water Electrolysis Current Density Spans at Various Water Flows	30
17	Current Density Spans for Various Water/CO ₂ Ratios	31
18	Endurance Test Voltage Versus Time, Cell No. 7	32
19	Current Density Spans Before, During and After High Voltage Operation	36
20	Current Density Spans During Endurance Test, Cell No. 7	37
21	Endurance Test Voltage Versus Time, Cell No. 12	39
22	Current Density Spans During Endurance Test, Cell No. 12	41
23	Performance Expected by Incorporation of Various Tube Cell Design Modifications	43

LIST OF TABLES

<u>TABLE</u>		<u>PAGE</u>
1	Electrolyzer Tube Cell Design Characteristics	6
2	O ₂ Purity Versus Current Density	28
3	Cell No. 7 Endurance Test Data	34
4	Cell No. 12 Endurance Test Data	40

ACRONYMS

CRS	CO ₂ Reduction Subsystem
OGS	Oxygen Generation Subsystem
ORS	Oxygen Regeneration System
SEORS	Solid Electrolyte Oxygen Regeneration System
SX-1	One-Man, Self-Contained, Oxygen Regeneration System
TSA	Test Support Accessories

SUMMARY

A program to design, develop, fabricate and assemble a one-man, self-contained, Oxygen Regeneration System (SX-1) incorporating electrolyzer drums that were designed, developed, fabricated and tested under Contracts NAS2-2810, NAS2-4843 and NAS2-6412 was completed. The SX-1 is a preprototype engineering model designed to produce 0.952 kg (2.1 lb)/d of breathable oxygen from the electrolysis of metabolic carbon dioxide and water vapor. The SX-1 was successfully designed, fabricated and assembled.

A task to develop a solid electrolyte cell with improved sealing characteristics was initiated and successfully completed in lieu of the SX-1 testing activity which could not be performed because of electrolyzer drum leakage. The results of the electrolyzer cell development task are the subject of this report. An improved cell design, termed a tube cell, was designed, developed, fabricated and tested. Design concepts incorporated in the tube cell to improve its sealing capability included minimizing the number of seals per cell and moving seals to lower temperature regions.

The advanced tube cell design consists of one high temperature ceramic cement seal, one high temperature gasket seal and three low temperature silicone elastomer seals. The two high temperature seals in the tube cell design represent a significant improvement over the ten high temperature precious metal seals required by the electrolyzer drum design. For the tube cell design evaluated in this program, the solid electrolyte was 8 mole percent yttria-stabilized zirconium oxide slip cast into the shape of a tube with electrodes applied on the inside and outside surfaces.

A commercially-available technique for application of electrodes to the solid electrolyte cells was evaluated and shown to provide performance equal to the electrodes developed under Contracts NAS2-2810, NAS2-4843 and NAS2-6412. Based on this result and the considerable cost advantage of using the commercial electrode application technique, all the tube cells evaluated contained electrodes applied by the commercial technique.

A three-position test stand was designed, fabricated and assembled for evaluating and characterizing the performance of individual tube cells. The test stand was designed to permit the characterization of the tube cells for carbon dioxide electrolysis, water electrolysis and combined carbon dioxide/water electrolysis. The test stand contained the necessary instrumentation and controls to obtain the data required to characterize the performance of the tube cell, i.e., flow control and measurement, temperature control and measurement, pressure measurement and product gas analysis.

A parametric test program for characterizing the tube cell was successfully completed. The tube cell was tested over a range of operating conditions, including variable carbon dioxide/water feed gas ratios, feed gas pressures up to 81.3 cm (32 in) water anode-to-cathode differential pressures up to 81.3 cm (32 in) water operating temperatures from 1023 to 1253 K (750 to 980 C), operating current densities up to 538 mA/cm² (500 ASF) and finally feed gas flow rates from 20 to 300 cm³/min (0.7 x 10⁻³ to 10.6 x 10⁻³ cfm).

The parametric test results demonstrated that the solid electrolyte tube cell could be successfully operated with feed gas pressures and anode-to-cathode differential pressures up to 108.2 kPa (15.7 psid), and that adequate performance could be attained at the following operating conditions: temperature 1233 K (960 C), water or carbon dioxide feed gas flow rate 150 cm³/min (5.3 x 10⁻³ cfm), anode-to-cathode differential pressure up to 7 kPa (1 psid), feed gas pressure 108 kPa (1 psig), and current density 97 mA/cm² (90 ASF). The parametric testing also revealed that the tube cells can successfully perform with any carbon dioxide/water feed gas mixture.

A carbon dioxide electrolysis endurance test was conducted on the tube cell configuration. One tube cell was successfully tested for 200 days operating at 97 mA/cm² (90 ASF). The oxygen produced contained less than 1.5% carbon dioxide and no detectable carbon monoxide for the entire test. A second tube cell incorporating a modified ceramic/metal seal was successfully operated for 21 days with less than 0.5% carbon dioxide and no detectable carbon monoxide in the product oxygen exhaust. In both endurance tests there was no increase in leak rate as a function of time like that characteristic of the electrolyzer drum design.

It is concluded that the tube cell design configuration will eliminate the process gas leakage problem characteristic of the electrolyzer drums. Continued development of the SX-1, involving the design, fabrication, assembly and testing of an electrolyzer module containing tube cells followed by integrating the module into the one-man system is recommended.

INTRODUCTION

There is a need for systems that can recover oxygen (O₂) from metabolically-produced carbon dioxide (CO₂) for future extended duration manned spaceflights. Such a system could decrease payload weight by reducing the need for stored O₂ at launch.

Several concepts for partially or completely performing this function have been proposed and studied. Some of these are the Fused Salt concept, the Solid Electrolyte concept, the Bosch Reactor concept, the Sabatier-Methane Dump concept, the Sabatier-Methane Decomposition⁽¹⁾ concept, and the Sabatier-Acetylene Dump concept. The results of a study⁽¹⁾ for evaluating and selecting life support systems for a 500-day nonresupply mission revealed that the most promising route for O₂ recovery from CO₂ was electrolysis using solid oxide electrolyzers and CO₂ Disproportionators with replaceable cartridges. Several features of the Solid Electrolyte concept led to its selection. The Solid Electrolyte Oxygen Regeneration System (SEORS) combines the function of two separate subsystems that are required in alternate Oxygen Regeneration Systems (ORS); a CO₂ Reduction Subsystem (CRS), such as a Bosch or Sabatier reactor and an Oxygen Generation Subsystem (OGS) (water electrolyzer). In the Solid Electrolyte concept, both CO₂ reduction and water electrolysis are carried out in the solid electrolyte electrolyzer cells. As a result, an ORS based on the Solid Electrolyte concept has a low equivalent weight, a minimum of interfaces, simplified instrumentation and an absence of condenser/separators for water removal.

(1) References cited at the end of this report.

Under National Aeronautics and Space Administration (NASA) Contract NAS2-7862, Life Systems, Inc. (LSI) designed, developed, fabricated and assembled a one-man, self-contained SEORS. However, leakage of the previously developed electrolyzer drums provided as Government-furnished equipment (GFE) to the program (NAS2-2810, NAS2-4843 and NAS2-6412) prevented testing of the system. The results of this effort were documented in an interim report. (2)

A task to develop a superior solid electrolyte cell was therefore initiated in lieu of the system test effort. This task involved the design, fabrication, assembly and testing of the advanced solid electrolyte cell. The design goal for the solid electrolyte cell was to eliminate the process gas leakage problem characteristic of the electrolyzer drums. These single-cell design, development and testing activities are the subject of this report.

The single-cell development program consisted of four major activities:

1. The development of a single cell design which minimized the number of high temperature seals and improved reliability relative to process gas leakage.
2. The evaluation of a new, cost-effective platinum electrode application technique and comparison of its electrochemical performance to that obtained with electrodes applied per NAS2-2810, NAS2-4843 and NAS2-6412 techniques.
3. The design, fabrication and assembly of a single cell test stand for evaluating the solid electrolyte single cells in the water electrolysis and CO₂ electrolysis operating modes.
4. The testing of the advanced solid electrolyte single cells which included checkout tests, parametric tests and an endurance test.

To accomplish the above, the program was divided into six tasks and program management functions. The specific objectives of the tasks were to:

1. Design, fabricate and assemble an advanced solid electrolyte single cell.
2. Design, fabricate, assemble and functionally check out the Test Support Accessories (TSA) for evaluating solid electrolyte single cells.
3. Implement a Product Assurance program to integrate maintainability, safety and quality assurance into the electrolyzer tube cell design and single cell test stand.
4. Conduct a test program consisting of test stand component checkout tests and calibrations, and single cell checkout, parametric and endurance tests.
5. Conduct a parallel technology program to evaluate an alternate platinum electrode application technique.

6. Incorporate the data management functions required to document and report the results of the development effort.

ELECTROLYZER TUBE CELL

The objective of the electrolyzer tube cell development effort was to design, fabricate and assemble an electrolyzer cell that reduces the number of high temperature seals as compared to the NAS2-6412 vintage electrolyzer drums and thereby increase the reliability of solid electrolyte cells relative to process gas leakage. This design objective was successfully accomplished. The following paragraphs describe the electrolyzer tube cell.

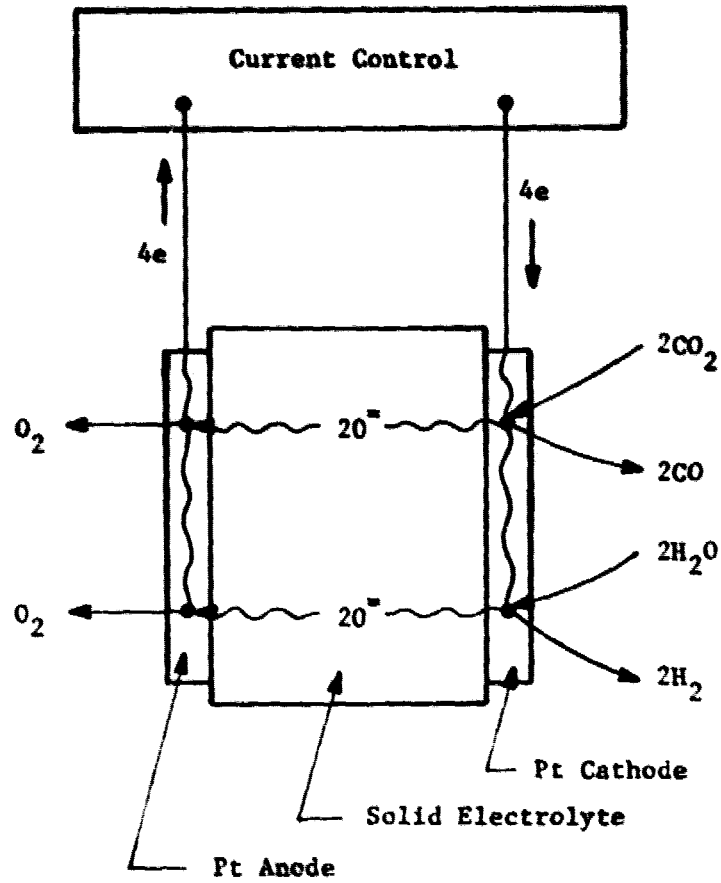
Electrolyzer Tube Cell Function and Reactions

The function of the solid electrolyte cell in an ORS is to electrolyze CO_2 into O_2 and carbon monoxide (CO) and to electrolyze water vapor into O_2 and hydrogen (H_2). A descriptive schematic of the cell operation along with the electrochemical reactions is shown in Figure 1. For CO_2 electrolysis, the feed gas (CO_2) enters the cathode compartment of the cell, where two moles of CO_2 react with four electrons to form two moles of CO and two oxide ions (O^-). The O^- ions migrate through the solid electrolyte and recombine at the anode to produce one mole of O_2 gas and release four electrons. For water electrolysis, water vapor enters the cathode compartment of the cell where two moles of water react with four electrons to form two moles of H_2 and two O^- ions. The O^- ions migrate through the solid electrolyte and react at the anode to produce one mole of O_2 and release four electrons.

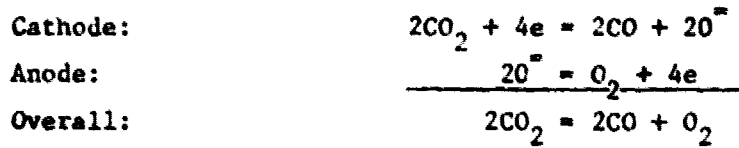
Electrolyzer Tube Cell Design Characteristics

The design characteristics of the electrolyzer tube cell are listed in Table 1. The most significant design characteristic in Table 1 is the number of high temperature seals. There are only two high temperature seals in the electrolyzer tube cell design. This compares to ten high temperature seals for the NAS2-6412 electrolyzer drum design. Figures 2 and 3 are sketches of the electrolyzer tube cell configuration and the electrolyzer drum configuration, respectively. In the sketches the high temperature seals are identified. The total number of seals for a one-man solid electrolyte ORS based on the respective electrolyzer cell designs are listed on each figure; 78 seals would be required with the electrolyzer tube cell design as compared to 320 seals for the electrolyzer drum design.

The type of high temperature seals employed in the electrolyzer tube cell design are much less prone to deterioration as a result of temperature excursions and extended operating life. The electrolyzer tube cells elevated temperature seals are a gasket seal and a ceramic cement seal as shown in Figure 2. The precious metal brazed seals characteristic of the electrolyzer drums have been completely eliminated. The precious metal seals suffered from recrystallization and grain growth of the braze material and a poor match of thermal coefficient of expansion between the precious metal and the ceramic materials.



CO₂ Electrolysis Reactions



H₂O Electrolysis Reactions

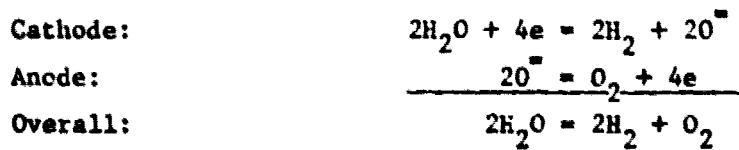


FIGURE 1 DESCRIPTIVE SCHEMATIC OF CO₂ AND WATER ELECTROLYSIS REACTIONS

TABLE 1 ELECTROLYZER TUBE CELL DESIGN CHARACTERISTICS

Performance Characteristics

CO₂ Electrolysis

Working Fluid Flow Rate ^(a)	CO ₂
Mass, kg/d (lb/d)	0.020 (0.044)
Volume, lpm (cfm)	0.031 (1.09 x 10 ⁻³)
Operating Temperature, K (C)	1203 to 1233 (930 to 960)
Operating Current Density, mA/cm ² (ASF)	107 (100)
Product O ₂ Purity, % O ₂	>99.5

Water Electrolysis

Working Fluid Flow Rate ^(b)	Water Vapor
Mass, kg/d (lb/d)	8.1 x 10 ⁻³ (0.018)
Volume, lpm (cfm)	0.031 (1.09 x 10 ⁻³)
Operating Temperature, K (C)	1203 to 1233 (930 to 960)
Operating Current Density, mA/cm ² (ASF)	107 (100)
Product O ₂ Purity, % O ₂	>99.5

Physical Characteristics

Weight, kg ₃ (lb) ₃	0.9 (2.0)
Volume, cm ³ (in ³)	178.8 (10.9)
Number of High Temperature Seals	2
Electrode Active Area cm ² (in ²)	13.0 (2.0)

Material Characteristics

Nonmetallics	Yttria, Zirconia, Alumina, Calcium, Graphite, Silicon (RTV)
Metallics	304 Stainless Steel, Platinum, Gold, Palladium, Inconel, Chromel/Alumel

Electrical Characteristics

Voltage, VDC	1.8
Current, A	1.4
Power, W	2.5

(a) At operating temperature, density of CO₂ 1.81 x 10⁻⁴ g/cm³ (0.011 lb/ft³).

(b) At operating temperature, density of steam 4.48 x 10⁻⁴ g/cm³ (0.028 lb/ft³).

continued-

Table 1 - continued

INTERFACES

Mechanical

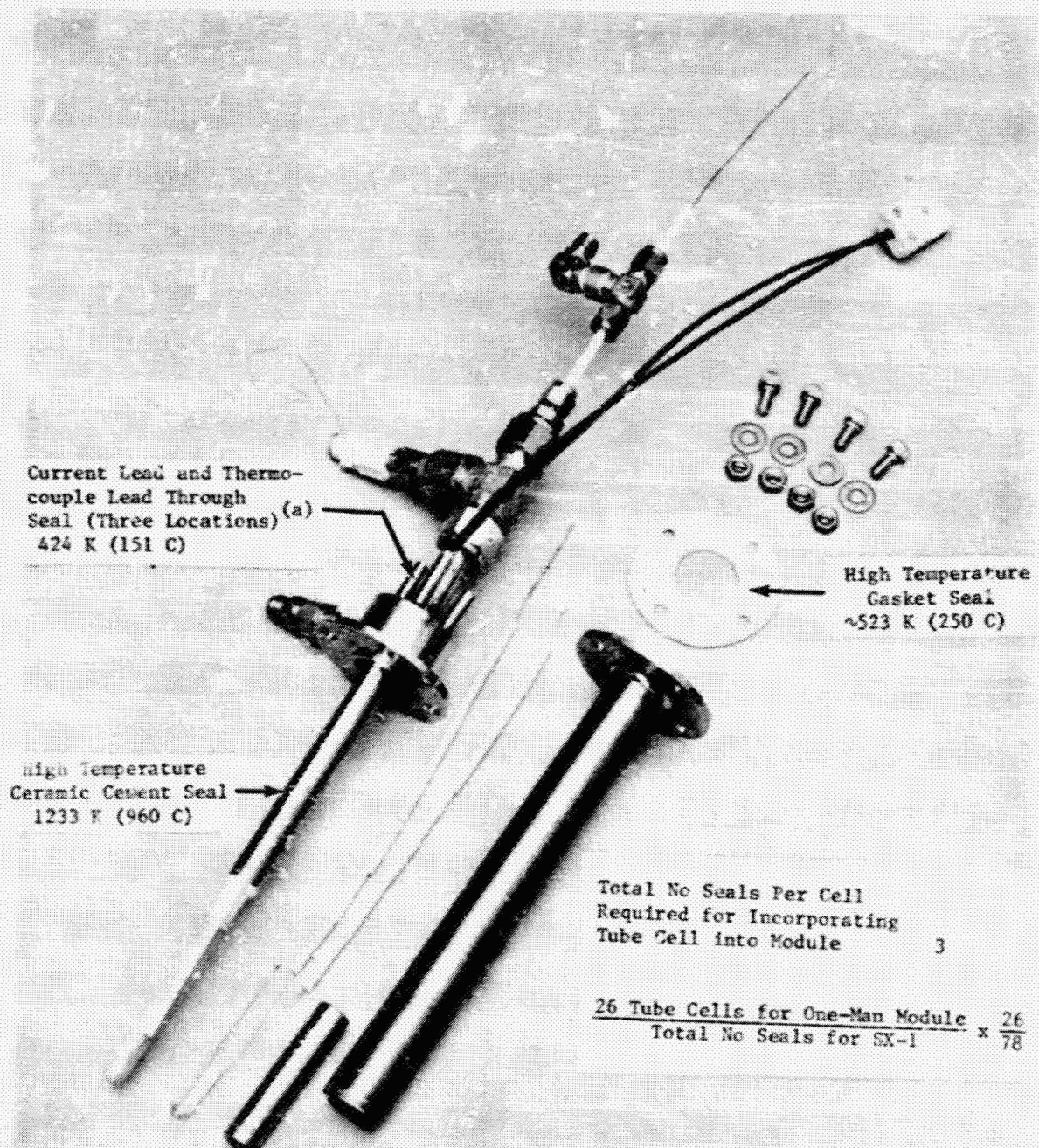
Feed Gas Inlet:
0.476 cm (0.187 in)
Swagelok, 300-3-316
Feed Gas Exhaust:
0.476 cm (0.187 in)
Swagelok, 300-R-8-316
Product O₂ Exhaust:
0.635 cm (0.250 in)
Swagelok, 400-6-316

Electrical

Leads:
Two conductor 500 series
cinch terminal block
Thermocouple:
K type thermocouple plug

Mounting

Placed inside muffle furnace
which is part of three position
single cell test stand



(a) Thermocouple lead throughs NOT needed for one-man module design. Hermetic sealed thermocouple wells in module housing will be used.

FIGURE 2 ELECTROLYZER TUBE CELL SEALS

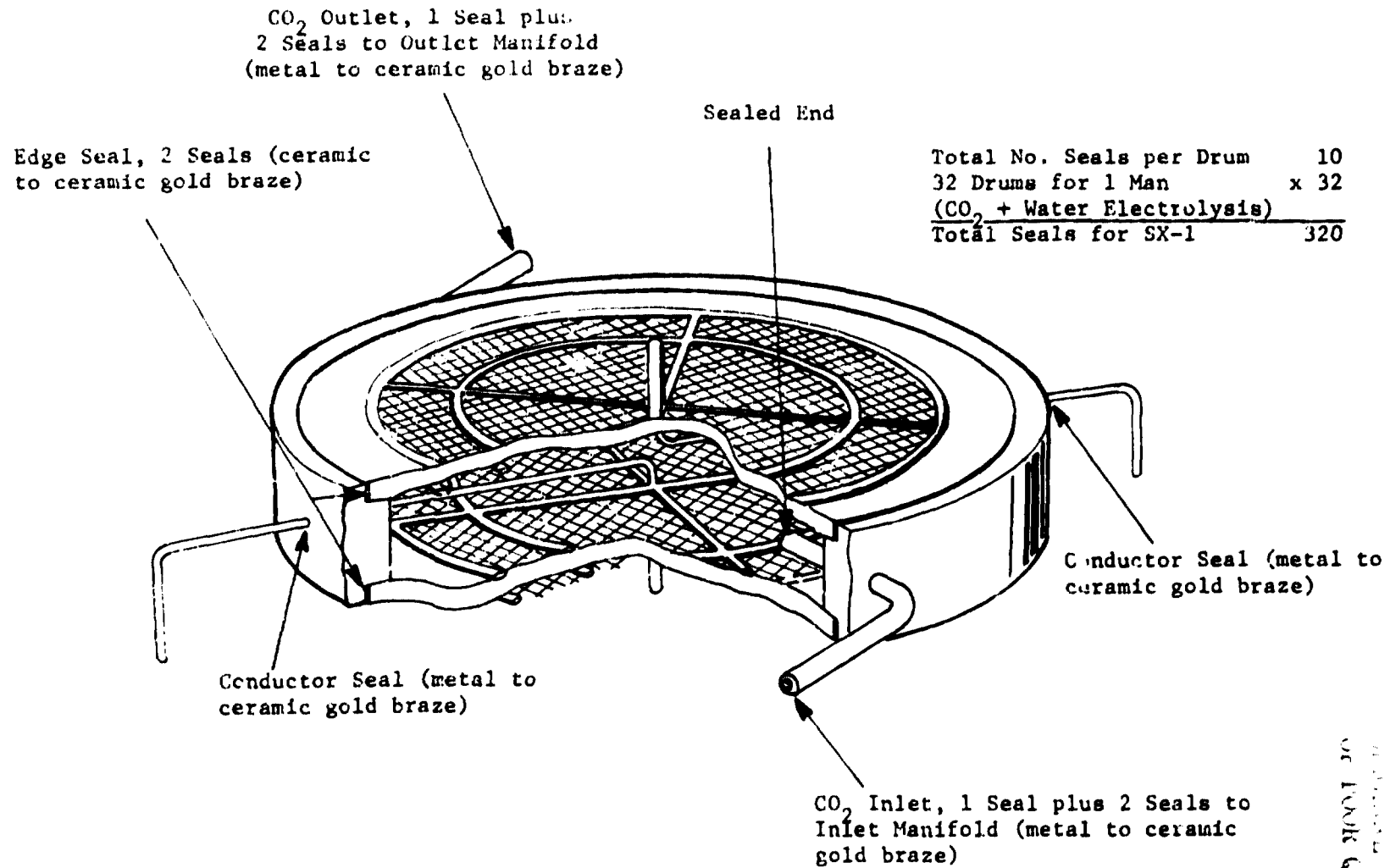


FIGURE 3 ELECTROLYZER DRUM DEPICTING NUMBER AND TYPE OF SEALS

THIS PAGE IS
OF POOR QUALITY

Life Systems, Inc.

Another characteristic of the electrolyzer tube cell design which decreases the probability of process gas leakage is the nature of the manufacturing process by which the electrolyte tube is produced. This process involves slip casting the tube followed by a high temperature fire. The resulting electrolyte tube structure is impermeable to gas in very thin cross sections. In comparison, the electrolyte discs used in the NAS2-6412 electrolyzer drums were sliced from hot pressed slugs. Since it is very difficult to achieve a completely non-porous slug in the hot press operation, subsequent slices from the slug can be porous, particularly slices from near the center of the slug. In order to minimize the electrolyte disc porosity the thickness of the solid electrolyte discs for the electrolyzer drums was maintained at greater than 0.15 cm (0.06 in).

In summary, an electrolyzer module based on tube cells will be more reliable relative to process gas leakage because (1) the number of high temperature seals has been reduced; (2) the type of high temperature seals are not prone to deterioration as a result of temperature excursions or extended operating life; and (3) the structure of the electrolyte material has an extremely low permeability.

Electrolyzer Tube Cell Description

The electrolyzer tube cell consists of a yttrium oxide (Y_2O_3) stabilized zirconium oxide (ZrO_2) solid electrolyte tube, feed gas manifolding, a product O_2 collection tube, anode and cathode current and voltage leads, thermocouples and the required gaskets, ceramic cement and fasteners for assembly. A photo of the electrolyzer tube cell is shown in Figure 4.

The components of the tube cell are identified in the photo. These are the solid electrolyte tube which is a 0.952 cm (0.375 in) outside diameter x 0.152 cm (0.060 in) wall thickness x 20.3 cm (8 in) long 8 mole percent Y_2O_3 stabilized ZrO_2 tube. The platinum electrodes are applied over a 6.35 cm (2.50 in) length at the bottom of the solid electrolyte tube on the inside and outside surfaces. The inlet gas is admitted to the tube cell via a tee fitting and stainless steel tubing and through a ceramic inlet tube which directs the feed gas to the bottom of the cell. The ceramic inlet tube also provides for the entry of the gold/3% palladium (Au/3% Pd) cathode lead wire which is threaded through the center of the ceramic tube. Three platinum (Pt) current distribution wires are brazed to the end of the Au/3% Pd lead. The three Pt current distribution wires are wrapped around the ceramic inlet tube and contact the Pt cathode 120 degrees apart. In effect, a press fit is obtained with the three Pt wires sandwiched tightly between the inside diameter of the electrolyte tube and the outside diameter of the ceramic inlet tube. A sketch of the ceramic inlet tube subassembly as positioned in the electrolyte tube is shown in Figure 5. The feed gas, after exiting at the bottom of the electrolyte tube, flows up around the ceramic inlet tube and reacts on the cathode of the tube cell which is the inner wall of the electrolyte tube. The cathode product gas proceeds up the tube and exits at the tee fitting as indicated. Oxide ions are transferred through the solid electrolyte material and react to form O_2 on the surface of the anode (outer wall of the solid electrolyte tube). The O_2 is collected in the O_2 compartment of the tube cell and exits through the O_2 vent. The anode current collector consists of a Pt wire which is

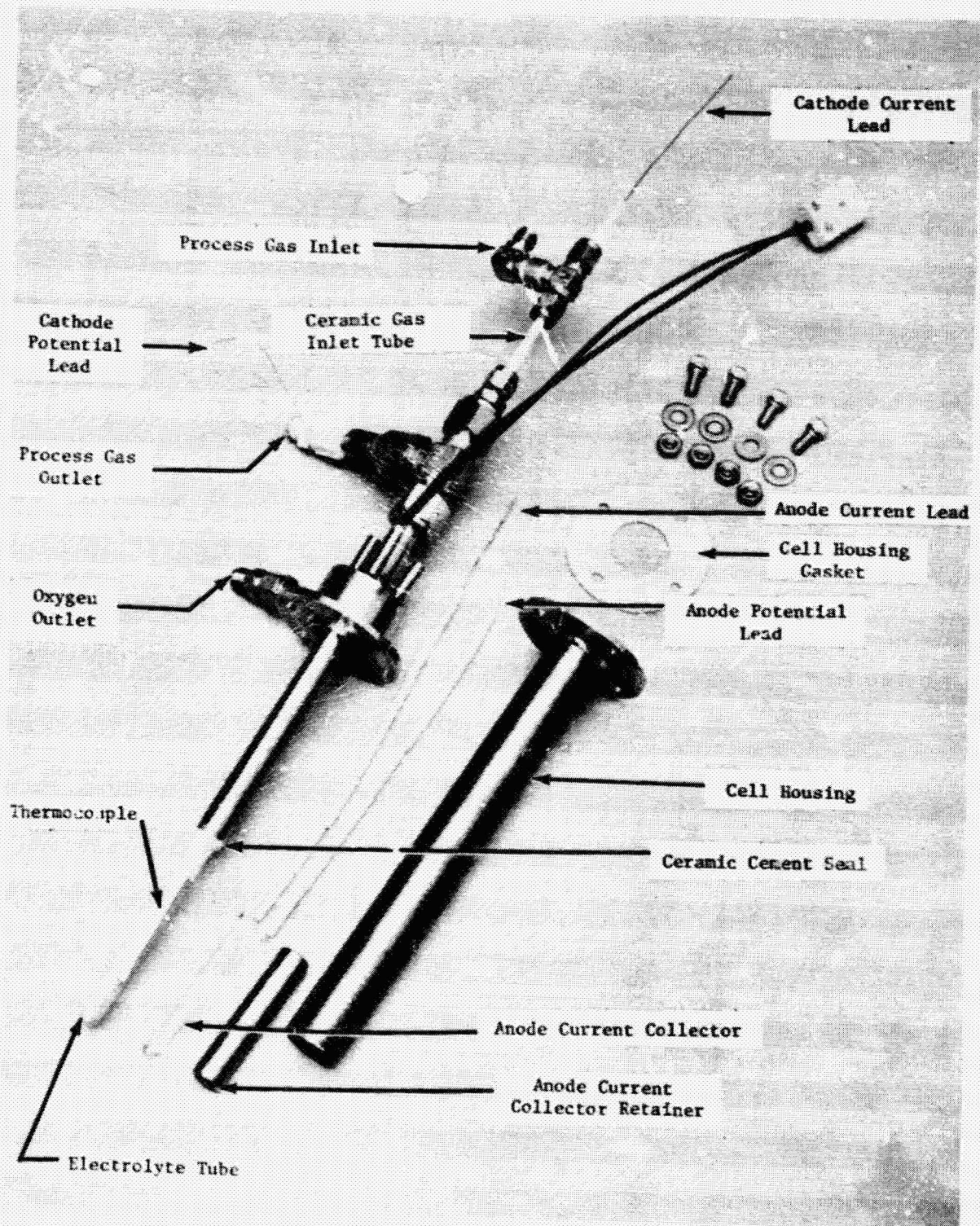


FIGURE 4 ELECTROLYZER TUBE CELL ASSEMBLY

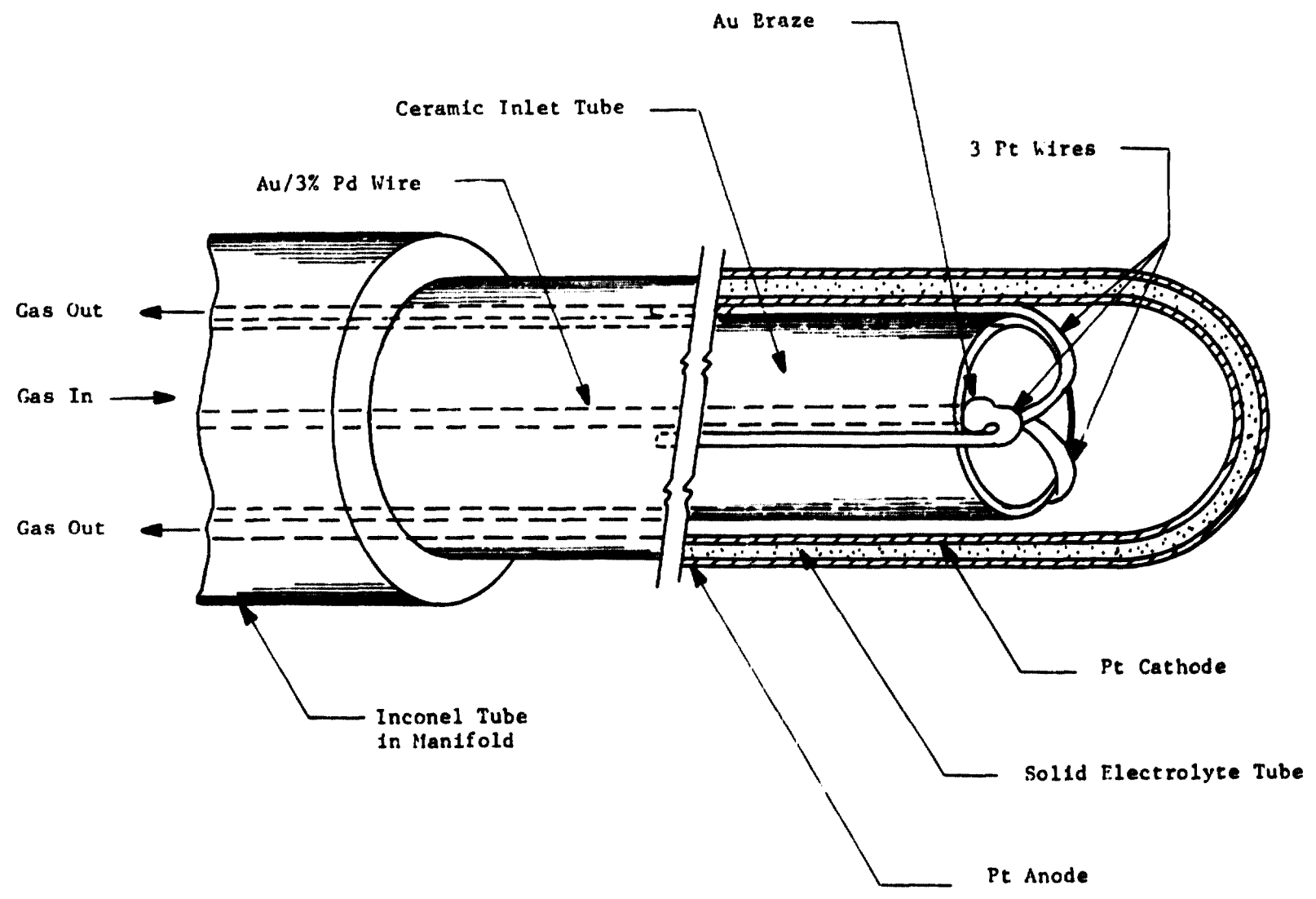


FIGURE 5 CERAMIC INLET TUBE SUBASSEMBLY AS POSITIONED IN ELECTROLYTE TUBE

sandwiched between the outside diameter of the solid electrolyte tube and the inside diameter of a precision machined Inconel anode current collector retainer tube such that a press fit is obtained. The tube cell seals and their approximate operating temperature are indicated in Figure 2. There are two high temperature seals. The electrolyte tube is sealed along a 10.2 cm (4.0 in) seal length inside an Inconel tube using ceramic cement. The cell housing assembly and the collection tube assembly are sealed with a high temperature gasket. The remainder of the seals are accomplished in a cooler zone using ceramic cement, silicone cement or tube fittings.

TEST SUPPORT ACCESSORIES

The TSA designed and assembled for the program were a three-position single-cell test stand and an electrolyzer tube cell leak test apparatus. The single-cell test stand included a gas distribution network, a steam generator and a gas product monitor.

Single-Cell Test Stand

The schematic for the single-cell test stand is shown in Figure 6. The single-cell test stand was designed to allow the simultaneous independent operation of three electrolyzer tube cells. Two positions were designed for only CO₂ electrolysis operation while the third (test stand position one) was designed for operation with pure CO₂, pure steam or any ratio of the two.

Water is converted into steam in the steam generator (SG-1). The steam passes through filter (F7) and through a downstream pressure regulator (R3). The pressure regulator (R3) maintains a constant downstream steam pressure which is measured by pressure gage P5. Excess steam is vented through a variable orifice flow control valve (V7). The steam flow rate to the electrolyzer tube cell passes through another variable orifice flow control valve (V6). By controlling the temperature of the steam generator, the steam pressure and the positions of variable orifice valves V6 and V7, the steam flow rate to the electrolyzer cell can be adjusted between the required 20 to 120 cm³/min (0.7 x 10⁻³ to 4.2 x 10⁻³ cfm) for water vapor electrolysis testing. After passing through variable orifice valve V6, the steam is directed to valve V4 which is used to configure test stand position 1 for either steam or CO₂ electrolysis. For steam electrolysis, valve V5 remains closed and the steam proceeds to the electrolyzer cell (EC1) which is maintained in an oven at operating temperature using the oven's temperature control circuits. Both the H₂ and O₂ product gas is routed through a trap (T1) water column (WR1) and flowmeter (F1). The trap is used to protect the single cell from accidentally being exposed to water that is contained in the water column. The water column serves two purposes. It acts as a pressure regulator and pressure gauge. Conventional pressure regulators that accurately control pressures from 101 to 108 kPa (14.7 to 15.7 psia) with sufficient accuracy at low product gas flow rates are not commercially available. The water column concept is used to provide backpressure control by inserting the exit gas tube to various depths in the water bubble column. From the water column the product gas is routed through a soap bubble flowmeter which is an accurate device for measuring low flow rates.

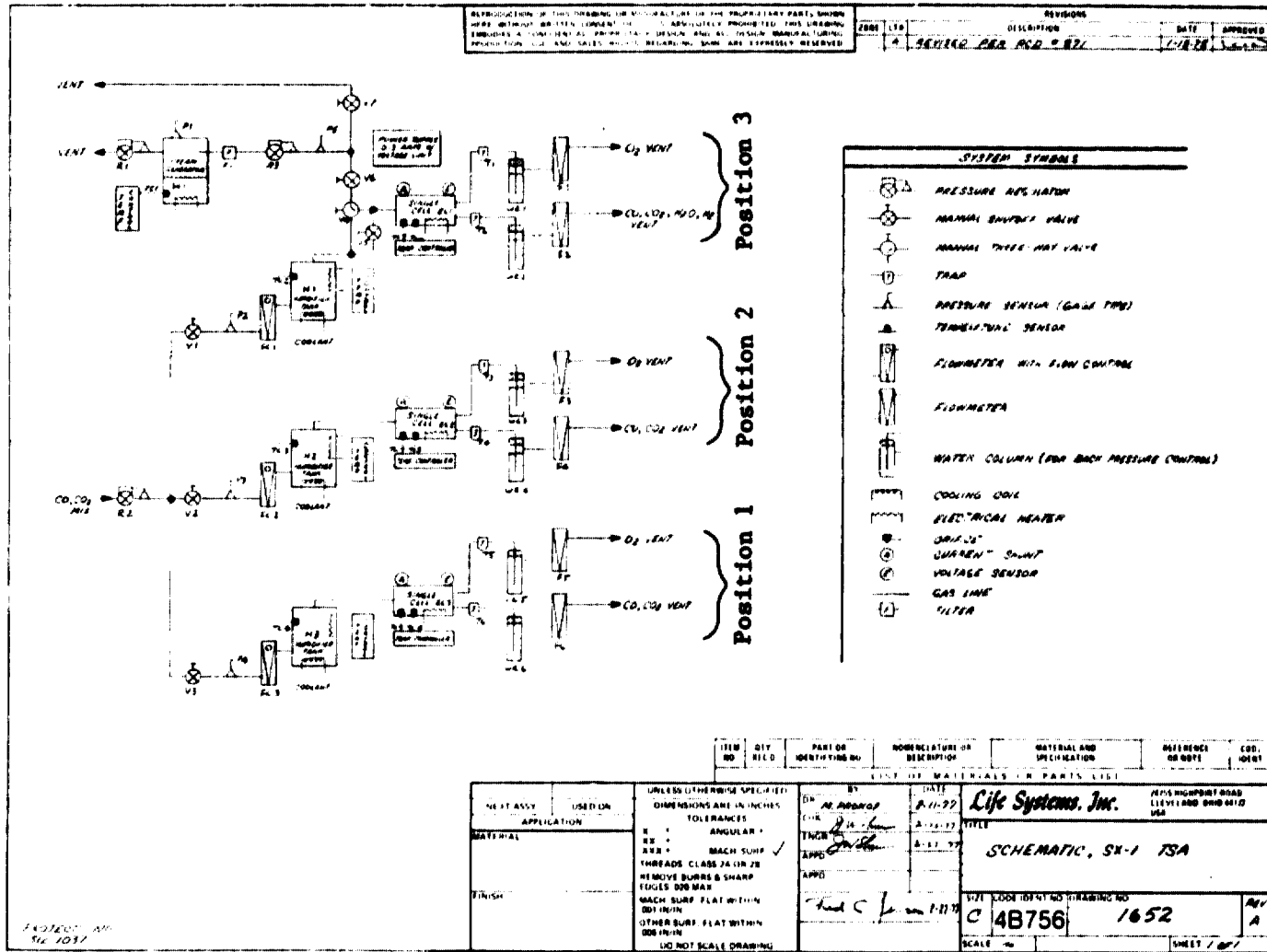


FIGURE 6 THREE-POSITION SINGLE CELL TEST STAND SCHEMATIC

ORIGINAL PAGE IS OF POOR QUALITY

All three positions of the test stand can operate in the CO₂ electrolysis mode. The CO₂ feed gas pressure is controlled by regulator R2. The feed gas then splits through three different routes through valves V1, V2 and V3. The feed gas pressure in each position is monitored by pressure gages P2, P3 and P4. Similarly, the gas flow is controlled by flow controllers FC1, FC2 and FC3. The flowmeters were calibrated and provide reproducible control. For test stand positions 1 and 3, flow can be controlled from 20 to 160 cm³/min (0.7 x 10⁻³ to 5.6 x 10⁻³ cfm). Test stand position 2 was fitted with a flowmeter which provides flow control up to 300 cm³/min (10.6 x 10⁻³ cfm). The gas is then directed through humidifier tanks H1, H2 and H3. The humidifier tank temperature is controlled in order to provide 3% water vapor in the feed gas stream. The 3% water is required to catalyze the CO₂ electrolysis reaction. (3) The gas exiting the humidifier tank is then directed into the single cell (EC2 and EC3) for test stand positions 2 and 3. For test stand position 1 to run in the CO₂ electrolysis mode the three-way valve, V4, must be in the CO₂ feed position and valve V5 closed. An additional provision in test stand position 1 is provided to allow running mixtures of steam and CO₂. This is done by positioning valve V4 in the steam configuration and by opening valve V5 to allow any combination of CO₂ and steam mixtures to be fed into the electrolyzer cell. The product gas pressure and flow control is similar for all three test stand positions.

A front view and rear view of the test stand are shown in Figures 7 and 8. The front view shows the instrument controls required for operation of the individual positions of the test stand. The front view photo of the test stand shows the CO₂ feed gas pressure gauges, flowmeters, oven temperature controllers, humidifier tank temperature controllers, steam line temperature controller, power supplies for each individual test stand position, current meter and voltage meter and accompanying switch which allows reading individual cell voltage and current parameters and the valves required for turning on and off CO₂ and steam flow. Also shown is the gas chromatograph and accompanying recorder which is used to determine product C₂ purity and the furnace for test stand position 3. The rear view reveals the feed gas humidifier, water traps, water columns, electrolyzer furnace for positions 1 and 2, the steam generator, the CO₂ feed gas supply and the gas chromatograph calibration gas supplies.

A Carle Analytical Gas Chromatograph 311 with a thermal conductivity detector and a 3 m (10 ft) Poropak Q capillary column was employed to determine CO₂, CO and H₂ in the O₂ product gas. Calibration curves were obtained using three standard gas mixtures. The recorder used was a Fisher Recordall Series 5000, or a Hewlett Packard, Moseley 7101B strip chart recorder with a built-in peak area integrator.

The test stand incorporates several safety features. The test stand is designed to shut down for high electrolyzer cell temperature, high steam generator temperature and for power failures. In addition, the power supplies have a voltage limit which allows control of the maximum voltage that can be applied to the electrolyzer tube cells.

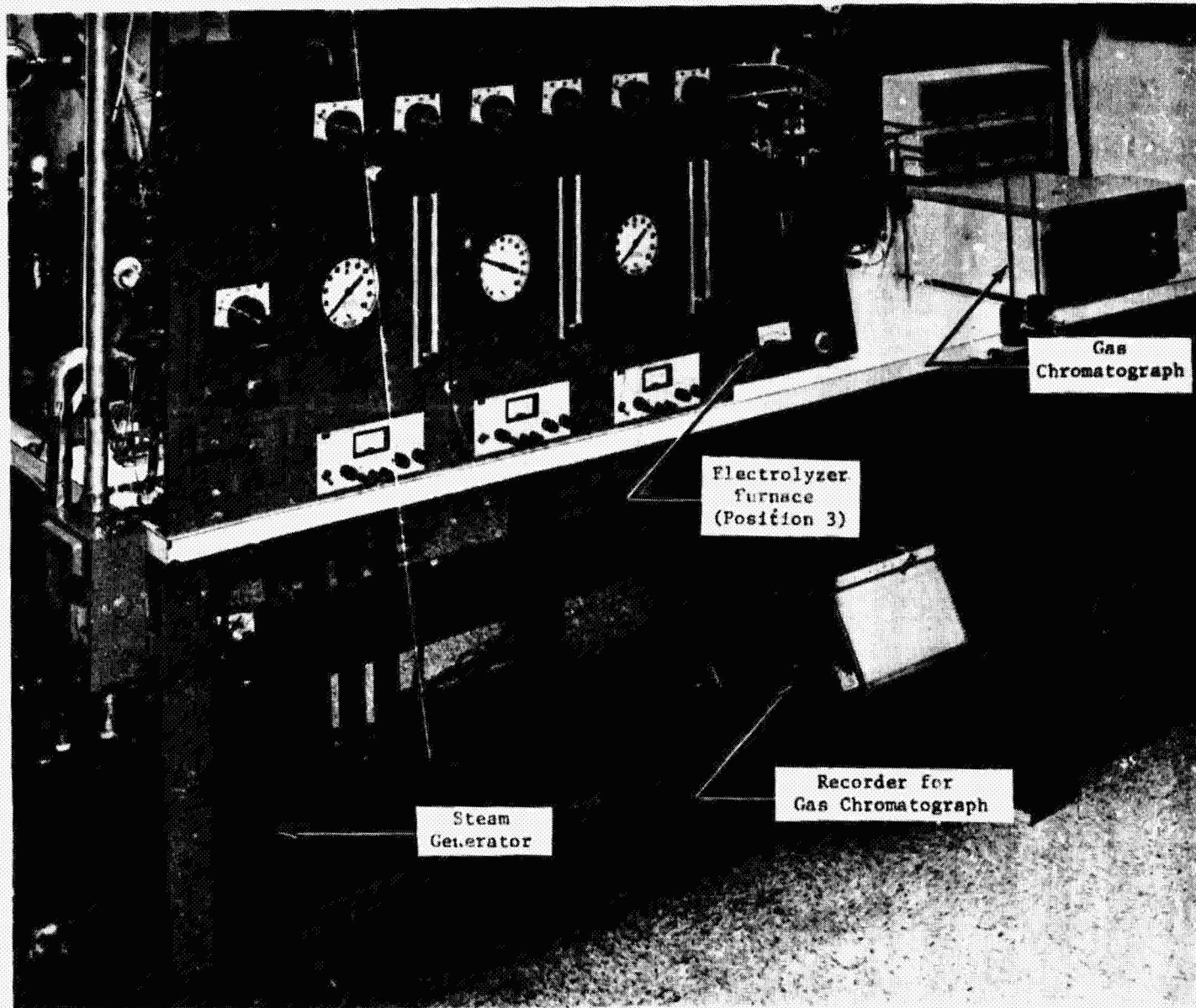


FIGURE 7 SINGLE CELL TEST STAND, FRONT VIEW

ORIGINAL PAGE IS
OF UNCLASSIFIED

ORIGINAL PAGE IS
OF POOR QUALITY

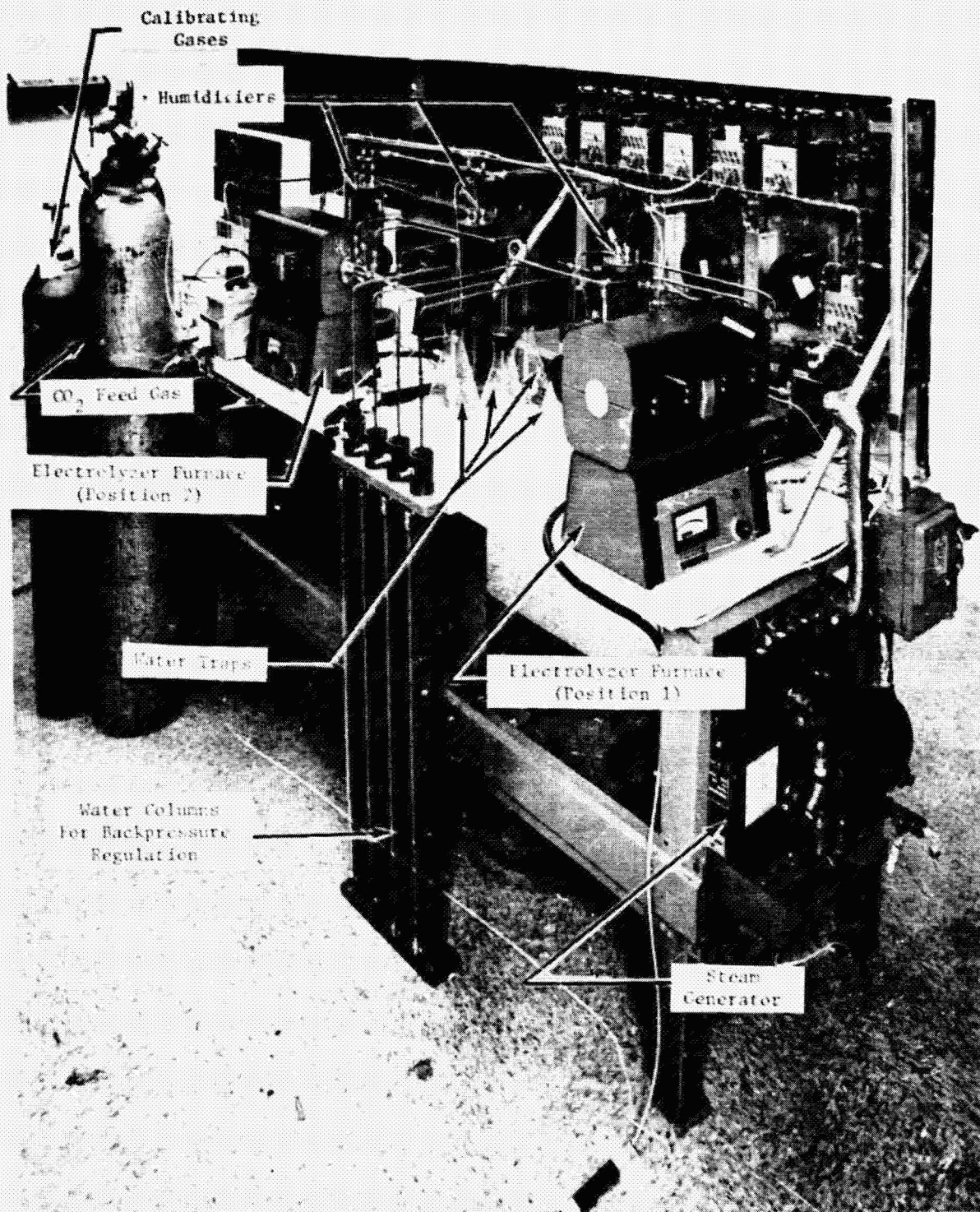


FIGURE 8 SINGLE CELL TEST STAND, REAR VIEW

Electrolyzer Tube Cell Leak Test Apparatus

A schematic of the leak test apparatus is presented in Figure 9. Nitrogen (N_2) pressure of 25 cm (10 in) water is applied to the tube cell using pressure regulator PR1 and valve V1. The pressure is measured with water manometer P1. For performing the leak test the N_2 gas supply is shut off using valve V1 and the pressure drop (water manometer P1) is measured as a function of time. If the pressure decreases greater than 2.5 cm (1.0 in) water in ten minutes the cell fails the leak test.

PROGRAM TESTING

A test program was completed to characterize the electrolyzer tube cell, with special emphasis on determining the reliability of the tube cell seals over time and on determining the cell's electrochemical operating characteristics. The test program consisted of checkout tests, parametric tests and an endurance test.

Electrolyzer Tube Cell Checkout Tests

The electrolyzer tube cell checkout tests included performing a leak test and current density span on each assembled cell. An additional checkout test was performed only on the first electrolyzer tube cell assembled. This test involved determining the Y_2O_3 stabilized ZrO_2 solid electrolyte breakdown voltage.

Leak Tests

The principal reason for the development of the electrolyzer tube cell was to improve the high temperature seals between the anode and cathode compartments of the cell in order to minimize CO_2 and CO leakage into the product O_2 . Each electrolyzer tube cell assembled was subjected to a leak test performed at operating temperature.

Early in the program, tube cells were assembled by manually packing ceramic cement into the 10 cm (4 in) long seal area between the electrolyte tube and the Inconel tube of the manifold assembly. This arrangement passed leak tests that were developed for electrolyzer drums.⁽⁴⁾ An improved ceramic cement vibration packing technique was developed during this program which resulted in a more uniform and a higher density packing of the ceramic cement in the seal zone and thereby produced a better seal. Using the vibration packing technique, assembled electrolyzer tube cells easily passed the leak test designed for electrolyzer drums. As a result, a much more rigorous leak test procedure was developed for the tube cells. Cells assembled using the vibration packing technique exhibit a pressure decrease of less than 1.25 cm (0.5 in) water in 10 minutes with a 25 cm (10.0 in) water pressure differential across the cell.

Zirconium Oxide Breakdown Voltage

The maximum operational current density of the electrolyzer tube cell is an important parameter for optimizing the design of an ORS based on CO_2 + water electrolysis via solid electrolyte cells.

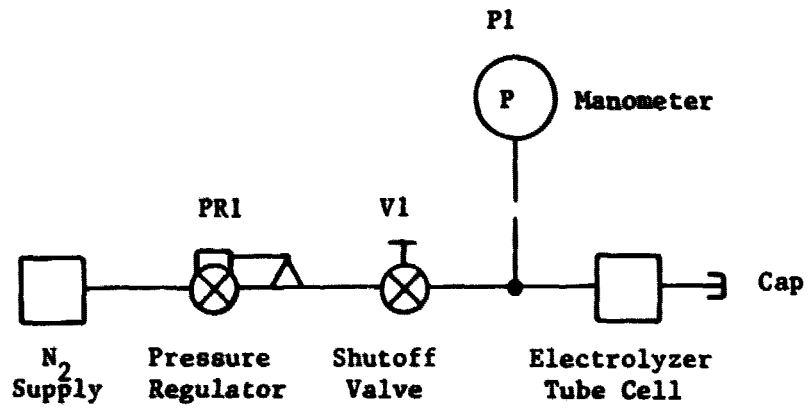


FIGURE 9 LEAK TEST APPARATUS SCHEMATIC

Higher operating current densities result in greater O_2 production per cell and therefore results in fewer cells per module and accompanying lower weight and volume of the ORS. At high current densities, however, the voltage required to sustain the electrochemical reactions (IR-free voltage^(a)) may exceed the reduction potential of the Y_2O_3 -stabilized ZrO_2 electrolyte.

Reduction of ZrO_2 to Zr would become a reaction competing with the desired CO_2 and/or water electrolysis process and if permitted to continue would result in the eventual destruction of the solid electrolyte. Hence, the maximum operational current density of a tube cell must be set such that its IR-free voltage is below the reduction potential of the electrolyte.

The electrolyte reduction or breakdown voltage of Y_2O_3 stabilized ZrO_2 was experimentally determined by purging the cathode compartment of an electrolyzer tube cell with pure N_2 gas, maintaining the anode in one atmosphere of O_2 and applying an increasing potential difference across the cell. The resulting current, was recorded. The results are presented in Figure 10 and indicate that electrolyte reduction commences near -1.0 V versus anode and increases rapidly above -1.2 V versus anode. From this result it was decided not to operate the electrolyzer tube cell above an IR-free voltage of 1.2 V.

The current/voltage curve commencing at approximately 0.5 V was obtained when CO_2 was fed into the cathode compartment and reduced at very low current densities.

A recent study⁽⁵⁾ indicates that the reaction taking place around 1.2 V could be the reversible formation of various Zr-Pt intermetallic compounds near the surface of the electrolyte on the cathode side of the tube cell. Requisites for the formation of these phases are highly polarizing conditions and very low O_2 activity, conditions found for both CO_2 and water electrolysis at the cathode.

The formation of these intermetallic compounds should not interfere with the electrolysis of the feed gas but since the electrolyte is multi-phased the potential of the cathode becomes independent of the feed gas composition and dependent on the percentage of Zr in the various Zr-Pt phases. The irreversible reduction potential of ZrO_2 was calculated, using thermodynamic data, to be 2.22 V.⁽⁶⁾ This is safely above the 1.2 V maximum IR-free voltage set for the electrolyzer tube cells.

CO_2 Electrolysis Current Density Spans

Current density versus voltage data for CO_2 electrolysis at current densities up to 484 mA/cm^2 (450 ASF) was obtained for all the electrolyzer tube cells assembled. A typical result is presented in Figure 11. Both terminal voltage and IR-free voltage are plotted versus current density. The difference in the

(a) The passage of current through a solid electrolyte cell requires a voltage to produce the desired electrochemical reaction (IR-Free voltage) plus an additional voltage to overcome cell resistance (IR voltage). The IR voltage must be eliminated when determining the electrochemical reduction potential of ZrO_2 .

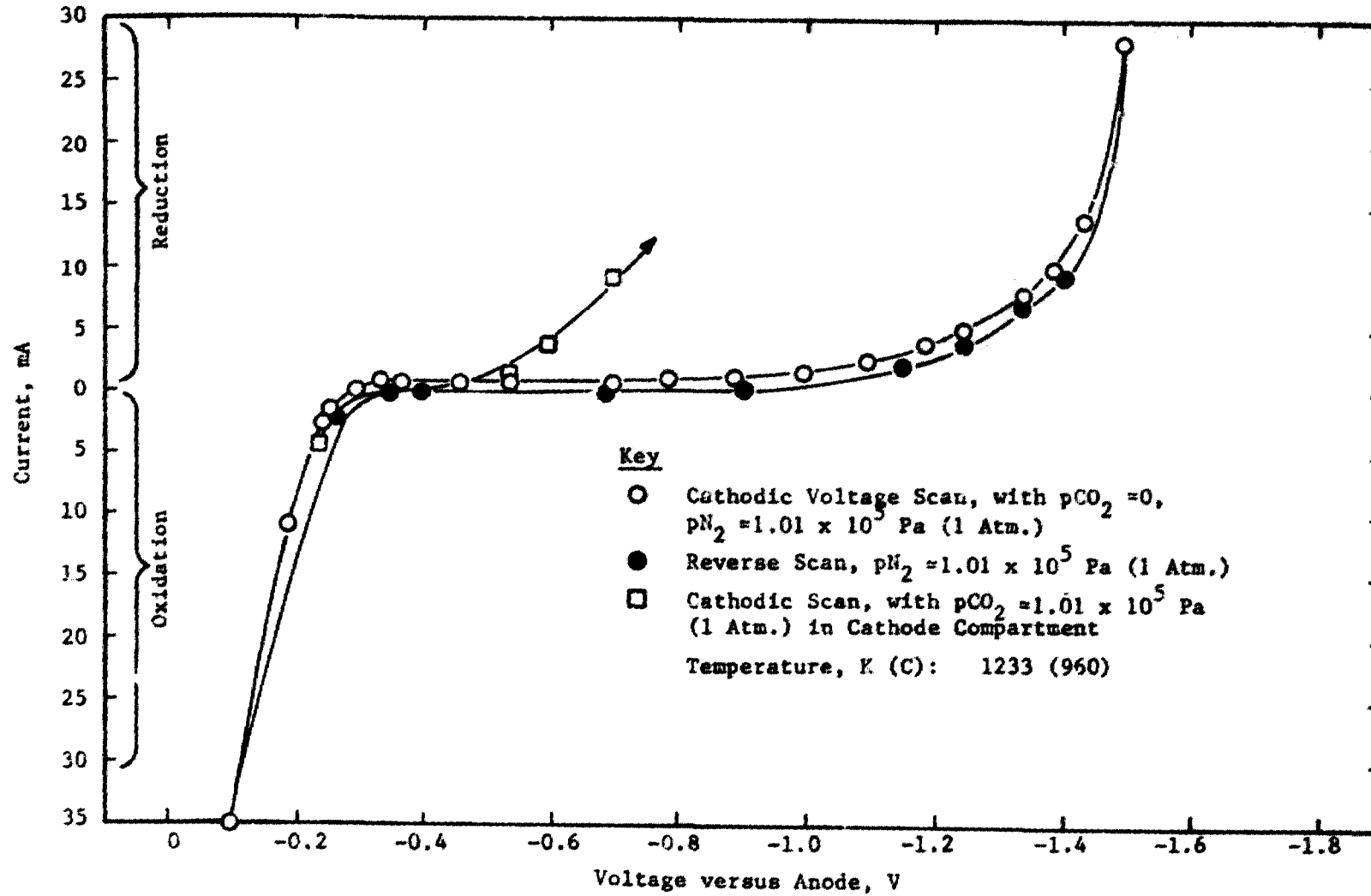


FIGURE 10 YTTRIA STABILIZED ZIRCONIUM OXIDE BREAKDOWN VOLTAGE

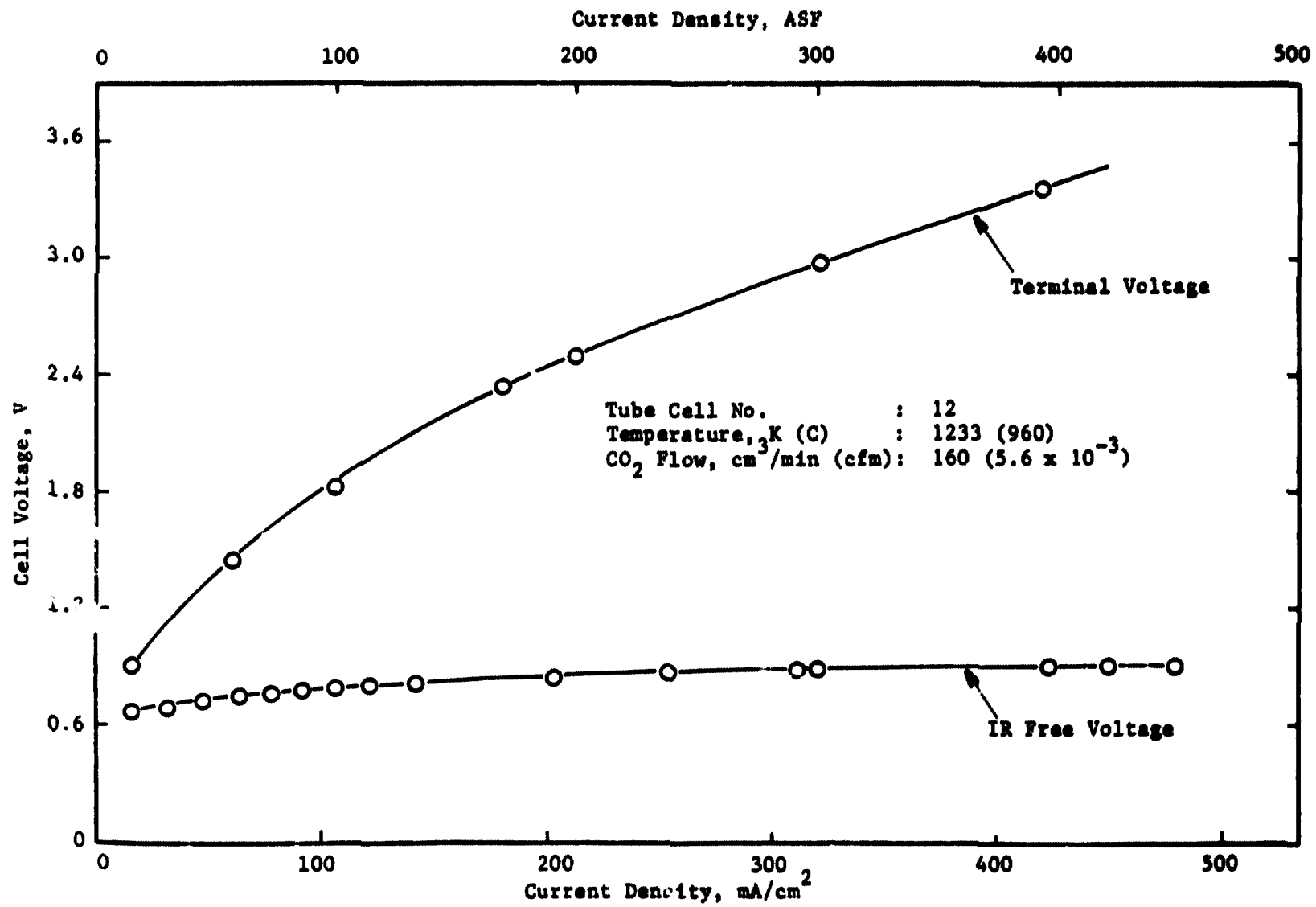


FIGURE 11 TYPICAL CURRENT DENSITY SPAN, CO₂ ELECTROLYSIS

two curves is a measure of the total cell resistance which is approximately 0.66 ohms. Measurements using noncurrent-carrying potential leads indicate that approximately 0.24 ohms is directly attributable to the resistance of the Pt and Au/3% Pd current carrying wires.

The IR-free voltage at 484 mA/cm^2 (450 ASF) is 1.0 V indicating that higher current density operation may be feasible, at least for short times, without exceeding the electrolyte breakdown voltage.

Water Electrolysis Current Density Spans

Current density versus voltage data for water electrolysis was obtained and typical data is presented in Figure 12. By comparing Figures 11 and 12, it is evident that the tube cells exhibit a similar behavior for both CO_2 and water electrolysis. Resistance values are similar to those obtained for CO_2 electrolysis reported above. The shape of the IR-free voltage versus current density curve also indicates that current densities greater than 538 mA/cm^2 (500 ASF) could be applied without exceeding the electrolyte breakdown potential.

Parametric Testing

Various parametric tests were performed to define the optimum operating conditions for the electrolyzer tube cell. Tests to determine the effects of temperature, backpressure, feed gas flow rate and feed gas composition were conducted. The results of these tests are reported in the following paragraphs.

Effect of Operating Temperature

The terminal voltage of an electrolyzer tube cell operated at several constant current densities was obtained at various operating temperatures. The results reported in Figure 13, indicate that electrolyte resistance to ionic conduction increases significantly below 1200 K (927 C). Above this temperature increasing current collector resistance nearly balances decreasing electrolyte resistance and little effect is observed. The operating temperature range for electrolyzer tube cells with Y_2O_3 -stabilized ZrO_2 electrolyte was therefore selected to be 1200 to 1233 K (927 to 960 C).

Effects of Backpressure

Tests were conducted to determine the effects of backpressure on the electrochemical performance and on the leak rate of electrolyzer tube cells. No effect was observed on terminal or IR-free voltage when backpressures up to 81 cm (32 in) water were applied to the feed gas or product gas exit ports of the electrolyzer tube cell.

A test was conducted to determine the effect of anode to cathode differential pressure on the leak rate of an electrolyzer tube cell. A tube cell was operated at a constant current of 5.0 A while the CO_2 backpressure was increased to 81 cm (32 in) water. The product O_2 purity was measured using a gas chromatograph for pressure differentials of 0, 20 cm (8 in), 41 cm (16 in), 51 cm (20 in) and 81 cm (32 in) of water. The results are presented in Figure 14 and indicate that increasing backpressure does not produce a major increase in

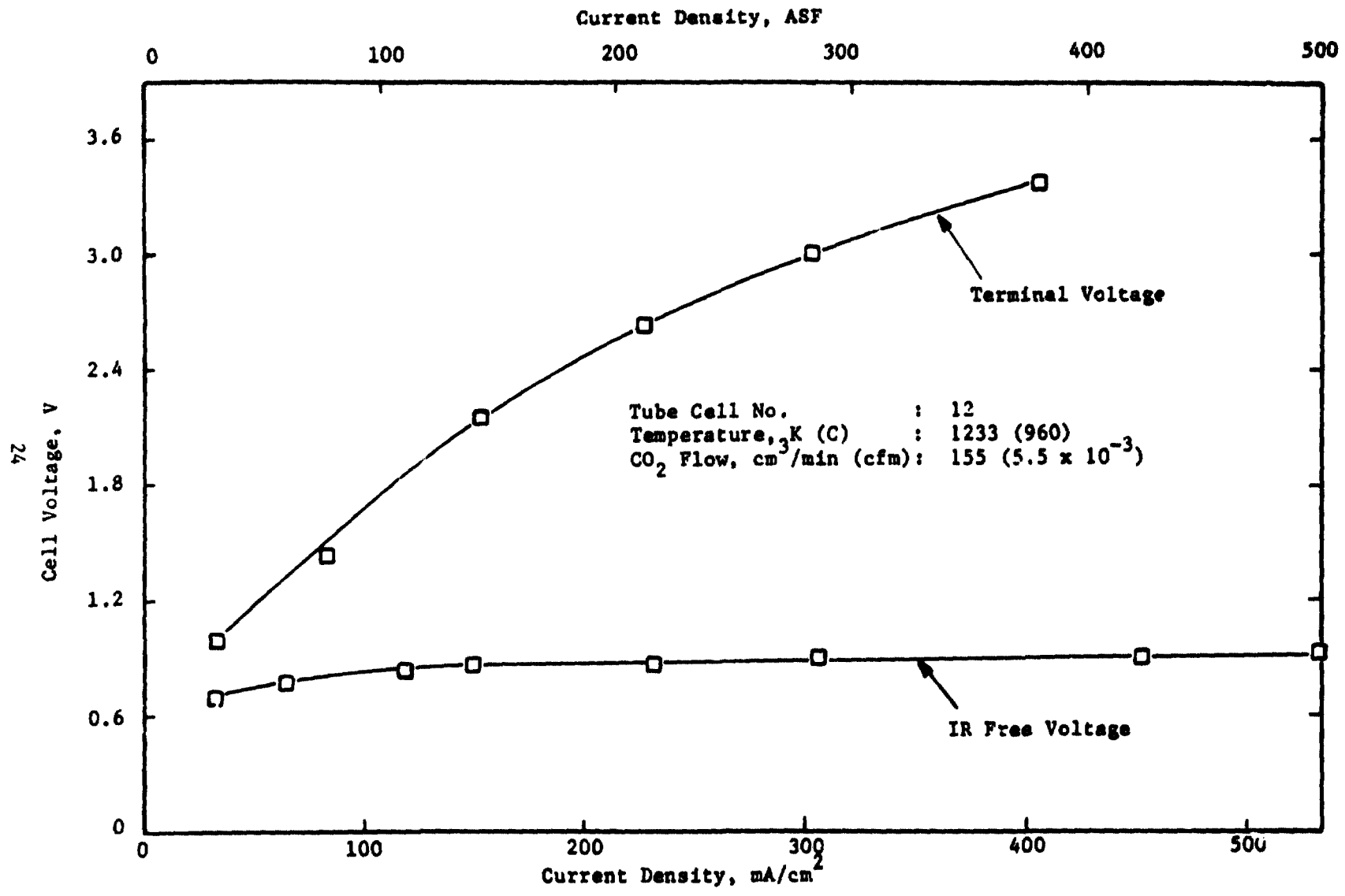


FIGURE 12 CURRENT DENSITY SPAN, WATER ELECTROLYSIS

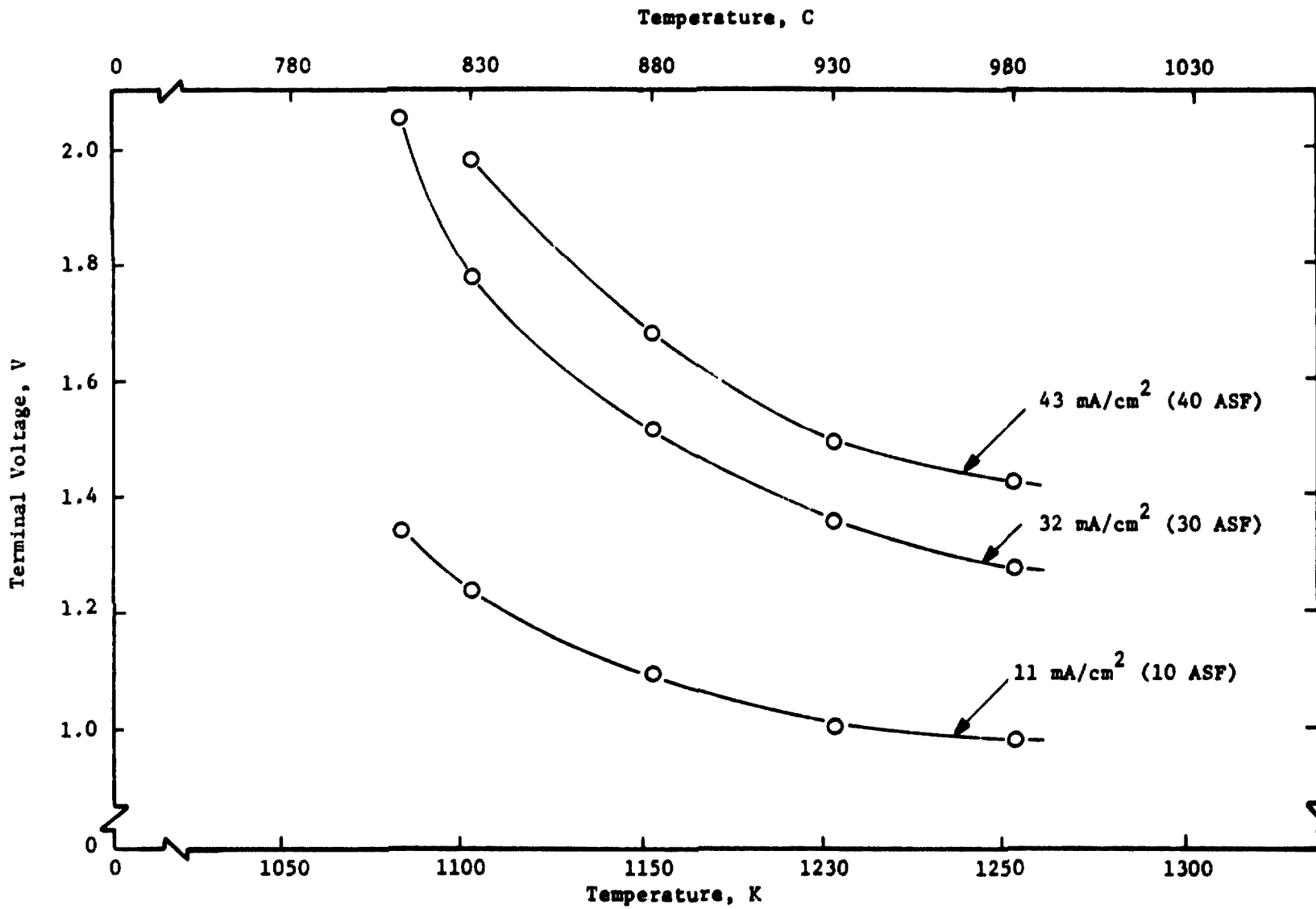


FIGURE 13 CELL VOLTAGE VERSUS OPERATING TEMPERATURE

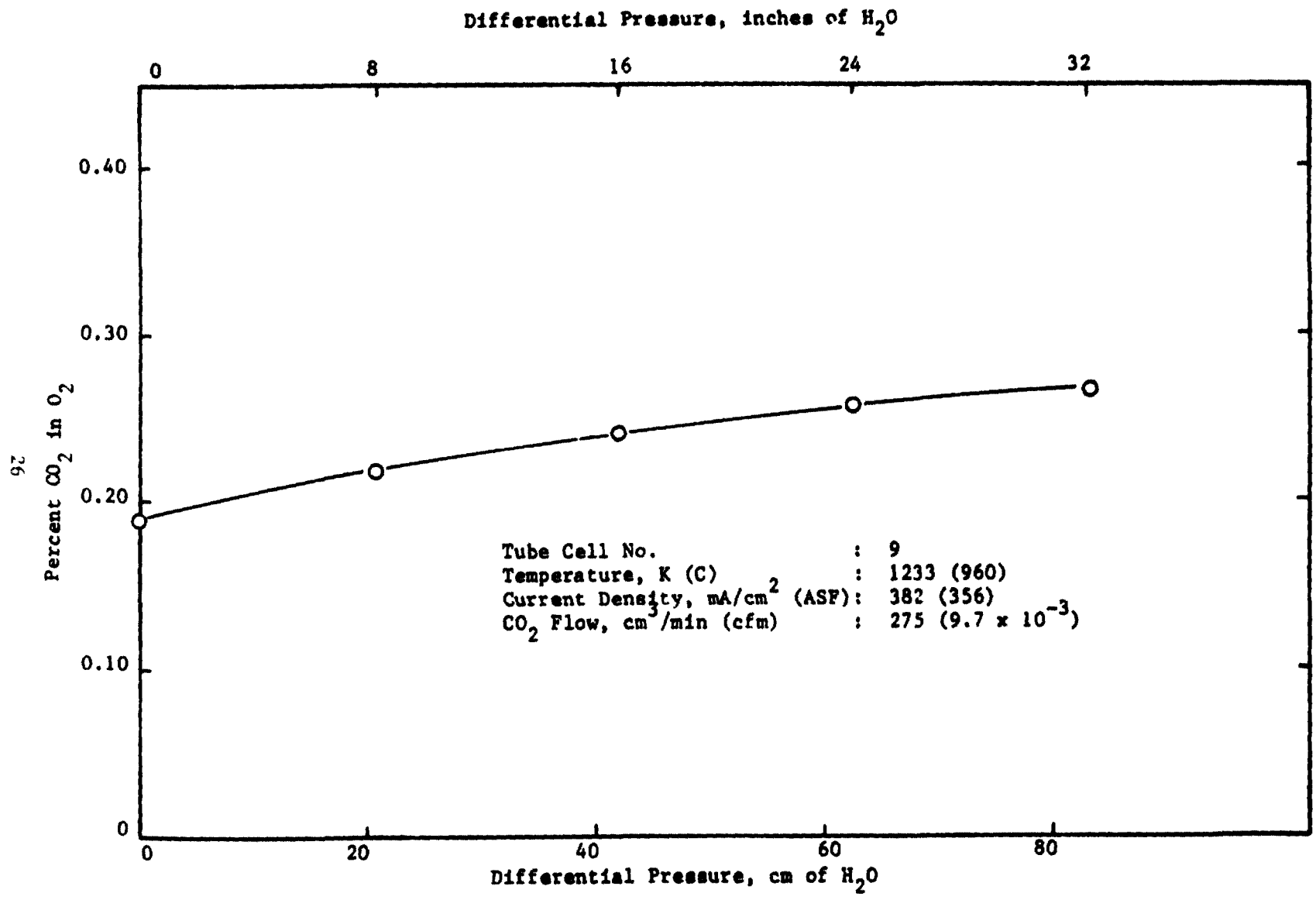


FIGURE 14 OXYGEN PURITY VERSUS DIFFERENTIAL PRESSURE

leak rate or catastrophic failure of the cell. Based on this test it was concluded that the tube cell can operate with pressure differentials of at least 6.9 kPa (1 psid) between anode and cathode compartments.

While performing these tests the percent CO₂ in product O₂ was determined as a function of current density. This data, presented in Table 2, points out that the effect of CO₂ leakage into the product O₂ can be minimized by operating the tube cells at higher current densities.

Effect of Feed Gas Flow Rate

The electrolyzer tube cell active area is 13 cm² (0.014 ft²). For 100% reduction at 108 mA/cm² (100 ASF) a CO₂ feed gas flow rate of approximately 10 cm³/min (3.5 x 10⁻⁵ cfm) is required. A test was conducted to determine the effect of feed gas flow rate on electrochemical performance of the tube cell. Current-voltage spans for various CO₂ and steam flow rates are presented in Figures 15 and 16, respectively.

The upturn of the curves indicates the commencement of concentration polarization. The electrodes become starved of feed gas at the higher current densities and increasing the flow rate does not lead to a corresponding decrease in voltage. The results possibly indicate a nonuniform distribution of feed gas across the electrodes. Improved gas distribution may allow higher current density operation for any given flow rate.

Effect of Feed Gas Composition on Performance

Current density versus voltage data for 100% CO₂, 100% water, a 0.6 mole ratio of water/CO₂ and a 1.2 mole ratio of water/CO₂ was obtained. The data, presented in Figure 17, indicates that at the test conditions cited there is little variation in performance between the feed gases. These results show that the solid electrolyte tube cell can be operated with any ratio of water and CO₂ feed gas.

Endurance Tests

An endurance test was initiated early in the test program to permit the acquisition of more than the contractually required 30 days of endurance test data. The first tube cell endurance tested (cell No. 7) was assembled employing Au/3% Pd current collector wires pressed to the cathode by a 1.25 cm (0.5 in) long Inconel 600 ring. The endurance test was begun August 6, 1977. The results of the endurance test are presented in Figure 18 and Table 3. After a preliminary break-in period where the terminal voltage gradually increased over a period of 27 days, a sudden large increase in terminal voltage occurred on the 27th day indicating some form of catastrophic failure. A check of IR-Free voltage, leak rate and product O₂ flow rate and purity all revealed no change in cell performance. A sudden drastic increase in cell resistance was the only apparent change.

The cell was operated intermittently for several days at high voltage, then slowly cooled to room temperature, disassembled and inspected.

TABLE 2 O₂ PURITY VERSUS CURRENT DENSITY

<u>Current,</u> <u>A</u>	<u>Current Density,</u> <u>mA/cm² (ASF)</u>	<u>%CO₂-in-O₂, %</u>	<u>Total O₂ Produced,</u> <u>cm³/min (cfm)</u>	<u>CO₂ Leak Rate,</u> <u>cm³/min (cfm)</u>
1.26	97 (90)	0.69	4.7 (1.6x10 ⁻⁴)	0.032 (1.1x10 ⁻⁶)
3.26	251 (233)	0.28	12.2 (4.3x10 ⁻⁴)	0.034 (1.2x10 ⁻⁶)
5.00	373 (347)	0.18	18.7 (6.6x10 ⁻⁴)	0.034 (1.2x10 ⁻⁶)

CO₂ Electrolysis, Cell No. 9

Temperature, ³K (C) : 1233 (960)
CO₂ Flow, cm³/min (cfm): 275 (9.7x10⁻³)

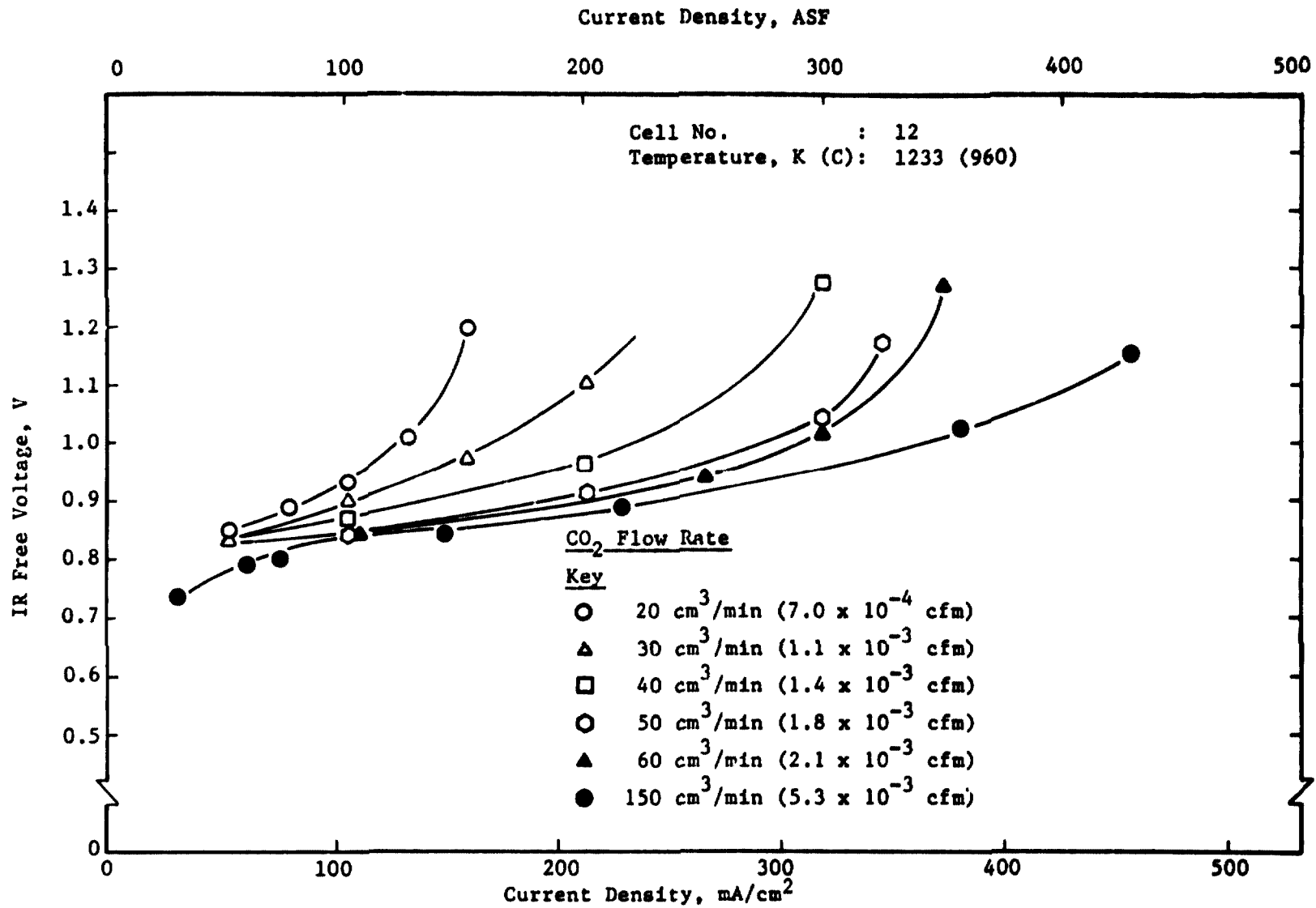


FIGURE 15 CO₂ ELECTROLYSIS CURRENT DENSITY SPANS AT VARIOUS CO₂ FLOWS

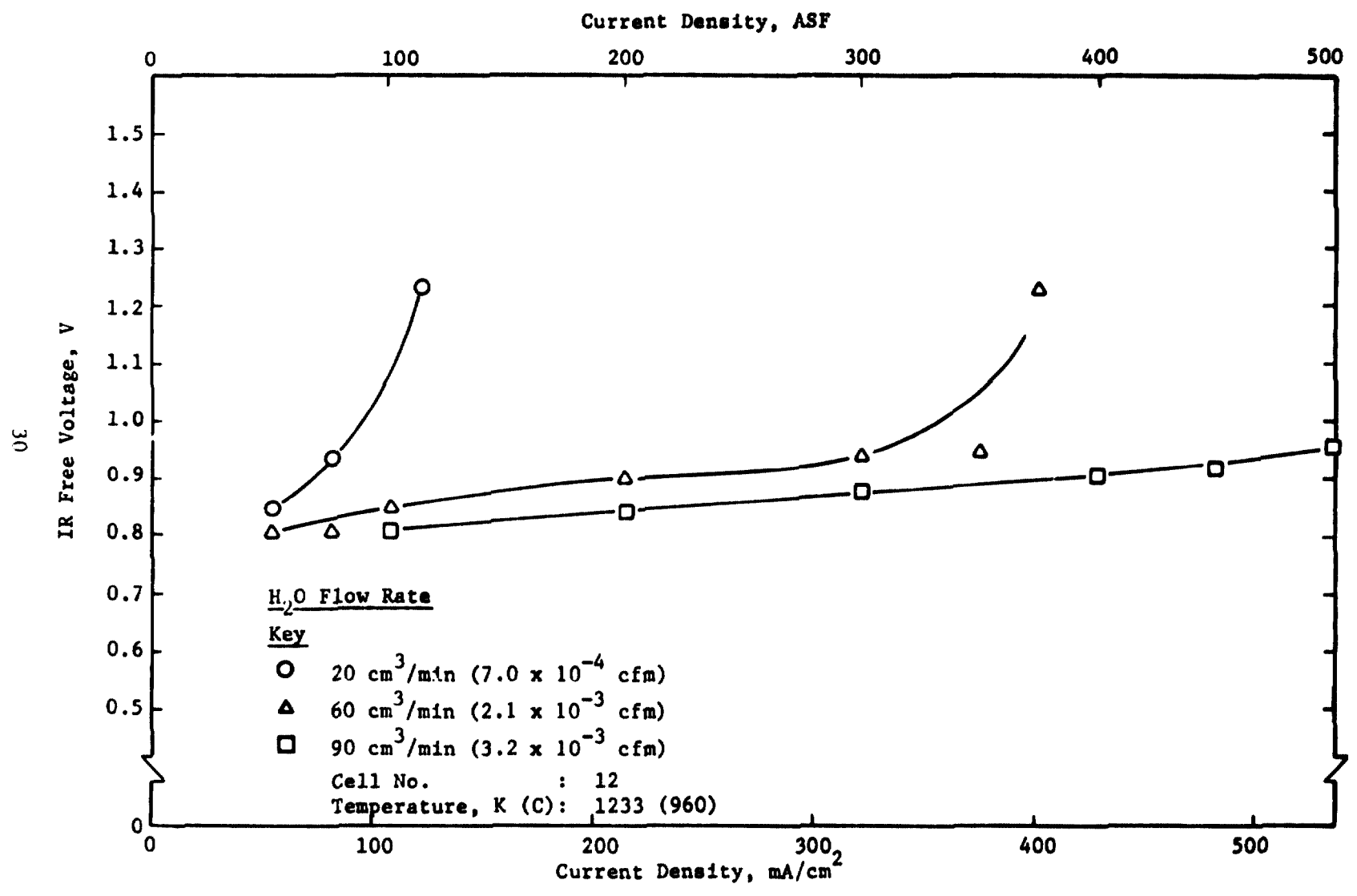


FIGURE 16 WATER ELECTROLYSIS CURRENT DENSITY SPANS AT VARIOUS WATER FLOWS

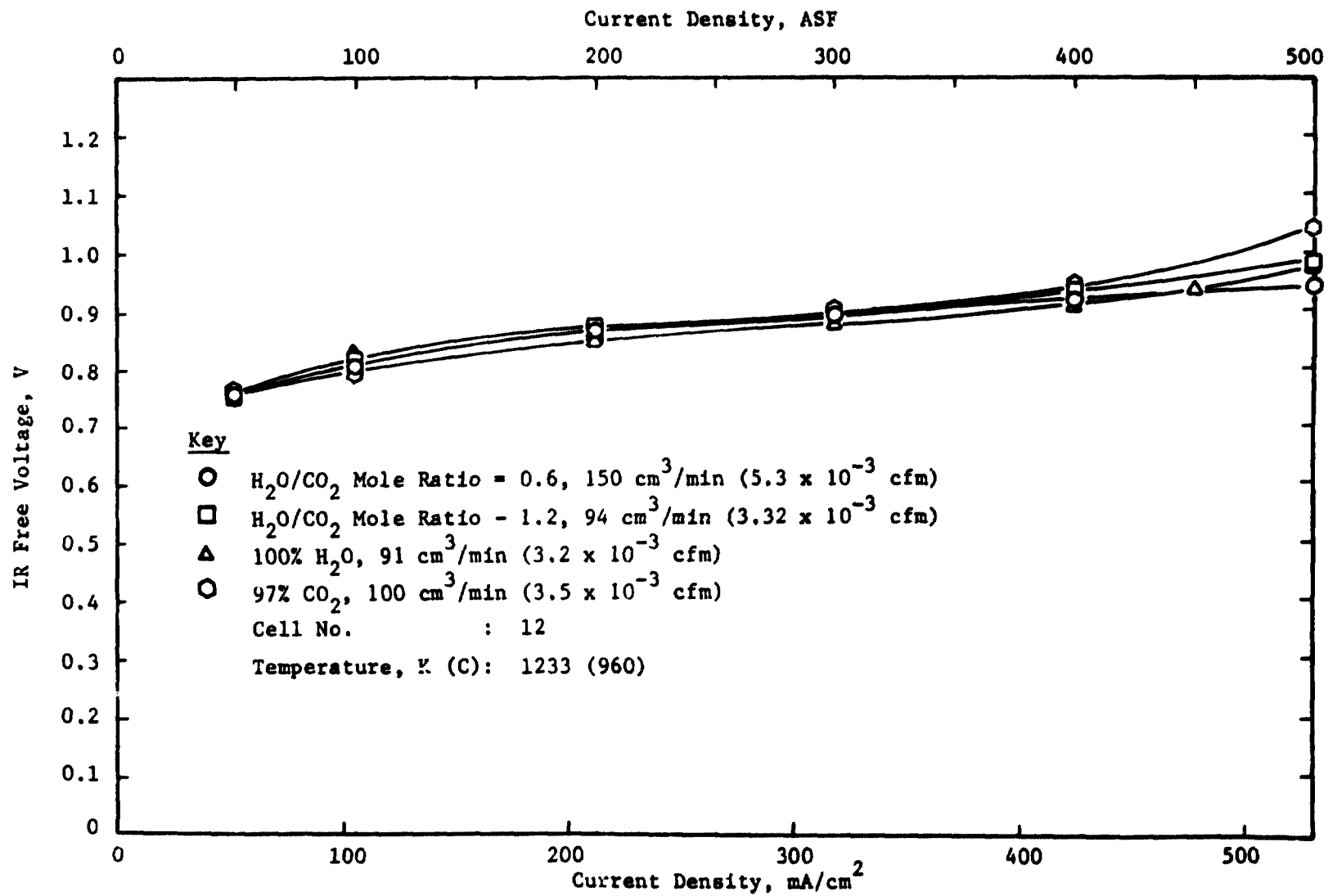


FIGURE 17 CURRENT DENSITY SPANS FOR VARIOUS WATER/CO₂ RATIOS

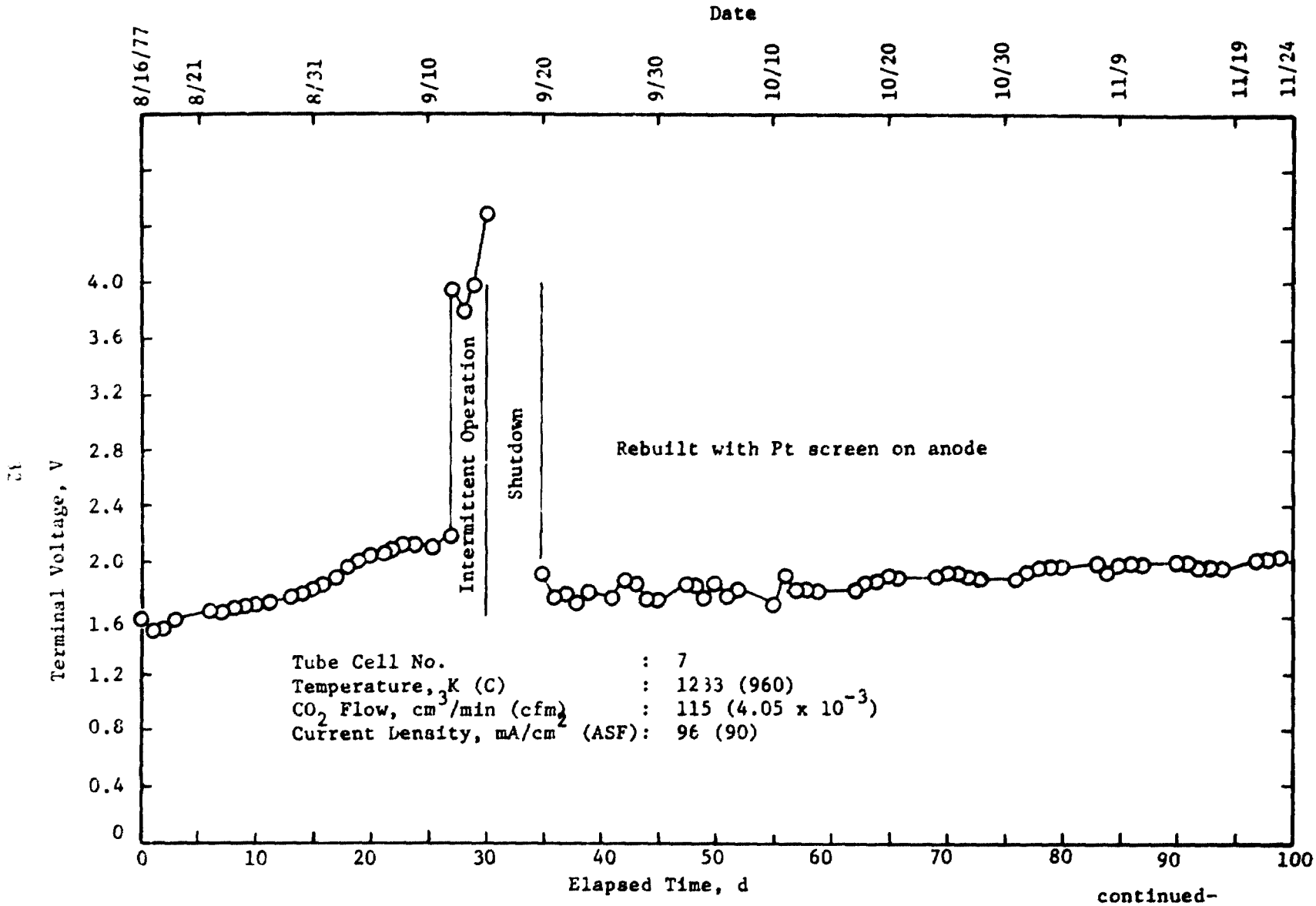


FIGURE 13 ENDURANCE TEST VOLTAGE VERSUS TIME, CELL NO. 7

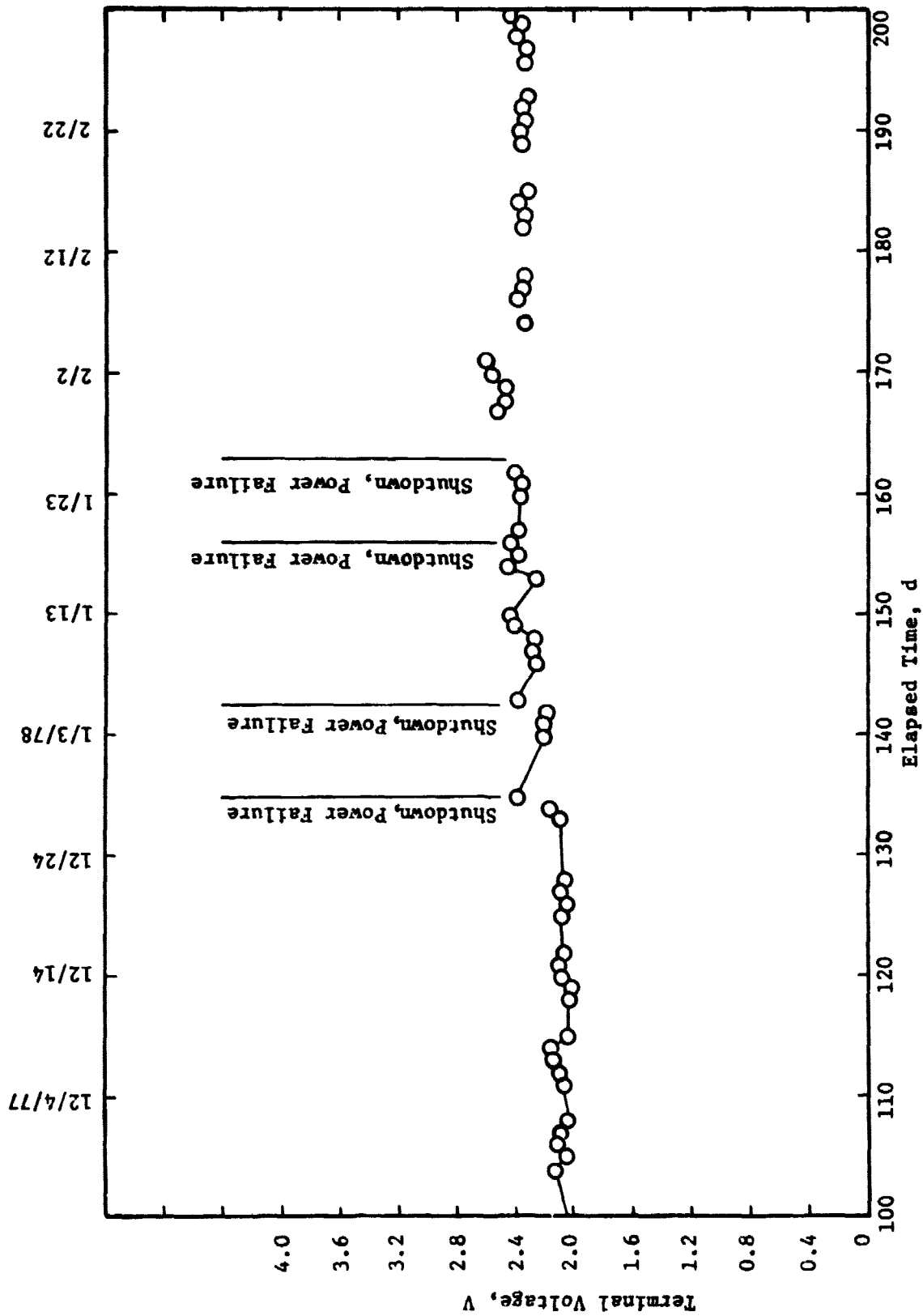


FIGURE 18 - continued

TABLE 3 CELL NO. 7 ENDURANCE TEST DATA

Cell No. 7
CO₂ Flow = 155 cm³/min (5.5 x 10⁻³ cfm)
Temperature = 1233 K (960 C)
Current Density = 97 mA/cm² (90 ASF)

<u>Day</u>	<u>Terminal Voltage</u>	<u>% CO₂-in-O₂</u>
1	1.55	N.T. (a)
10	1.70	N.T.
20	2.05	N.T.
29 (b)	3.78	0.66
35 (c)	1.92	1.57
36	1.75	1.35
48	1.83	1.28
59	1.79	N.T.
70	1.90	N.T.
77	1.95	1.40
83	1.99	1.32
90	2.00	1.28
99	2.05	1.48
108	2.07	1.40
115	2.04	1.56
125	2.07	1.57
137	2.21	1.57
143	2.25	1.49

(a) Data not taken.

(b) Cell shutdown after this data point.

(c) Cell rebuilt and back on test.

A visual inspection of the anode revealed loss of electrode material under the Au/3% Pd current collectors and the Au/3% Pd current collectors exhibited a grayish color at the electrode contact surface. The current collectors were only marginally in contact with some areas of the Pt electrode.

Disassembly of the cathode compartment revealed a similar, though less severe, loss of electrode material under the cathode current collectors.

Platinum from the electrode had migrated into and alloyed with the Au/3% Pd current collectors resulting in a gradual loss of contact between the electrode and current collector wires and a loss of electrode area. This led to a significant increase in current density in the area under the current collector wires and passivation of a large fraction of the electrode area. The higher localized current density resulted in a larger IR drop across the cell and accompanying high voltage shutdown.

The last data measurements before cell disassembly showed no degradation in electrochemical (IR-free voltage) performance, so it was decided to attempt to rebuild the cell.

The anode current collector wires were reinserted after rotating the assembly 60 degrees so that the Au/3% Pd wires were again in contact with the Pt electrode. In an effort to prevent future alloying problems of the Pt electrode with the Au/3% Pd current collector wires the cathode was wrapped with a thin platinum screen and the gold current collector wires were reapplied over the top of the screen. The Inconel 600 retaining ring was replaced with an Inconel 600 tube the length of the cathode. This configuration isolates the Pt cathode from the Au/3% Pd current collector by the Pt screen.

After rebuild the cell was reheated to the operating temperature and the endurance test was continued. Alloying had resulted in a loss of approximately 30% of the Pt electrodes. The current for the continuation of the endurance test was therefore reduced so as to maintain a 97 mA/cm² (90 ASF) current density based on the reduced electrode area.

Current density versus voltage spans representing performance before, during and after cell high voltage operation are presented in Figure 19. The results clearly show that the failure mechanism caused increases in IR polarization and that the electrochemical operation of the cell (IR-free voltage) did not degrade as a result of the failure.

The endurance test on the tube cell reached 200 total days of operation on the date of publication of this report. The endurance test is being continued under an IRAD Program. The 200 days included 175 days of continuous operation after rebuild. Both terminal voltage and IR-free voltage has gradually increased with time after the cell was rebuilt as shown in Figure 20 which contains current density spans at various times during the endurance test. These results imply a gradual increase in both overall cell resistance and electrochemical polarization. Such results may be explained by a gradual decrease in electrode surface area.

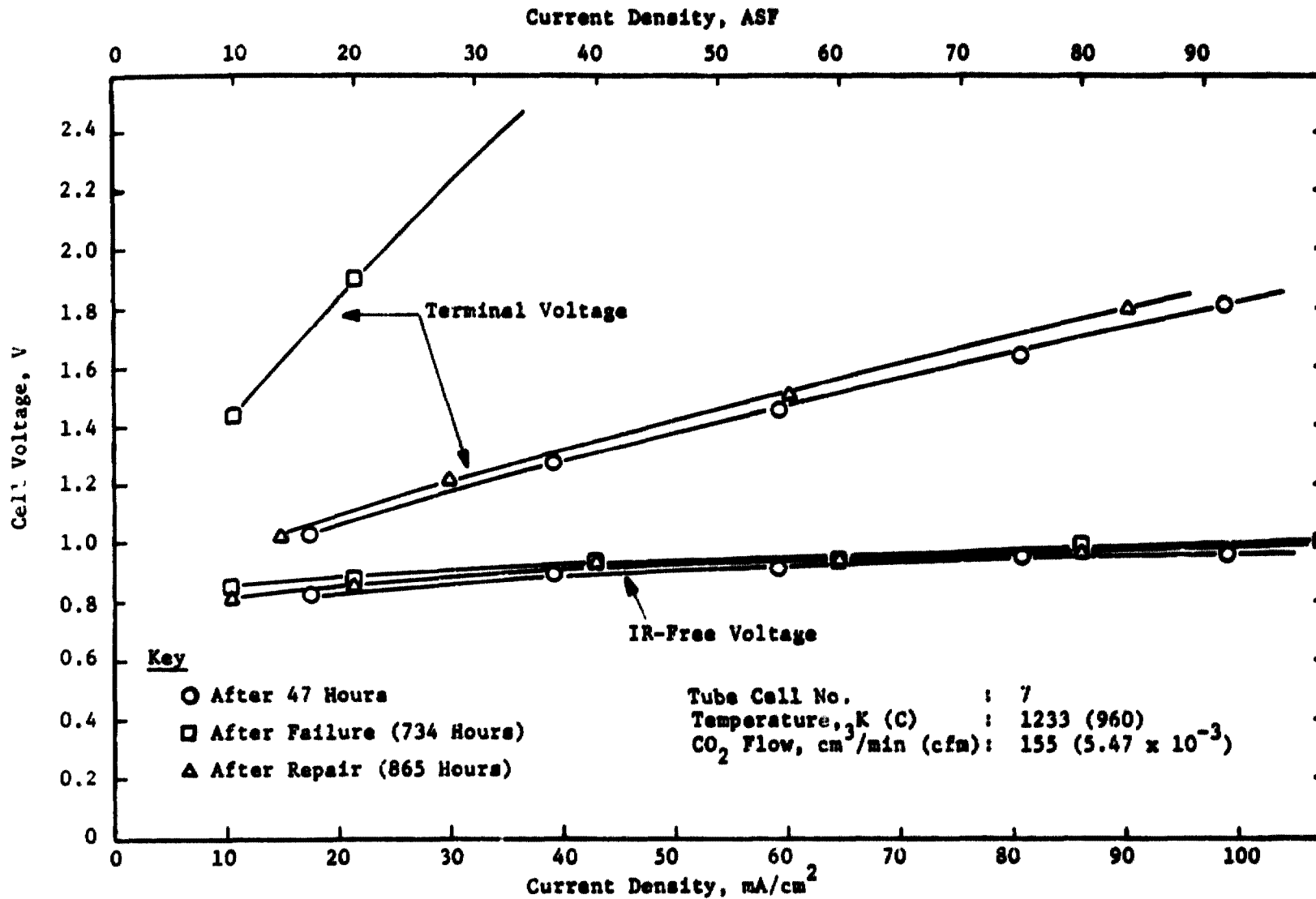


FIGURE 19 CURRENT DENSITY SPANS BEFORE, DURING AND AFTER HIGH VOLTAGE OPERATION

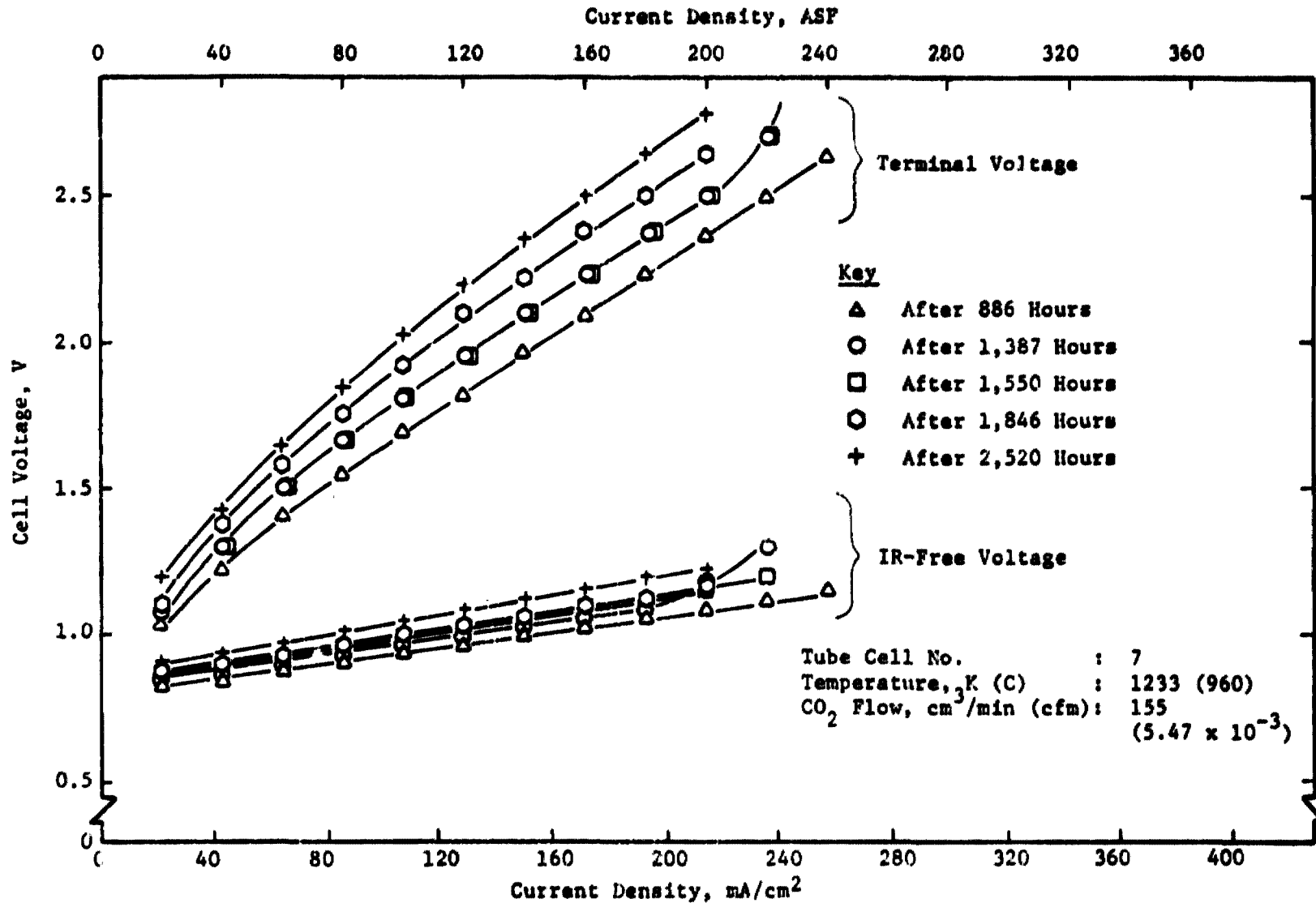


FIGURE 20 CURRENT DENSITY SPANS DURING ENDURANCE TEST, CELL NO. 7

During the endurance test the current efficiency remained at 100% within the accuracy of the measuring technique (see Table 3). Before the cell was rebuilt O_2 purity remained constant at 99.3% (or 0.7% CO_2 in O_2). After the rebuild, product gas purity remained at approximately 98.6% (or 1.4% CO_2 in O_2). The increase in leak rate can be attributed directly to the cooling down and rebuilding process.

A second endurance test was initiated employing cell No. 12 which was assembled with the improved vibration sealing technique and Pt current collector wires. This cell was previously operated intermittently over 39 days during which various parametric tests were performed. The purpose of this second endurance test was to demonstrate 215 mA/cm² (200 ASF) current density operation and low leak rate for an extended period of time. This cell was operated for 21 days with a current efficiency of approximately 100% and a leak rate below 0.2% CO_2 in O_2 . The results of this test are presented in Figure 21 and Table 4. Current density spans taken at various times during the endurance test are presented in Figure 22. A building power failure during which the cell cooled in an uncontrolled profile to room temperature caused the cell to be ruined by thermal shock. The uncontrolled cooling can be eliminated for future modules incorporating electrolyzer tube cells by designing the insulation such that cooling occurs with a profile of <3 K (3 C)/minute.

SUPPORTING TECHNOLOGY STUDIES

Three supporting technology study tasks were carried out during the program. These were (1) the development of an improved ceramic cement seal between the electrolyte tube and the Inconel manifold tube, (2) the evaluation of a commercial electrode application technique and (3) a study to determine the methods for decreasing the electrolyzer tube cell IR voltage losses.

Ceramic Cement Seal Development

The ceramic cement seal between the electrolyte tube and the Inconel tube underwent a significant improvement during the course of the program. Initially the ceramic cement was applied by coating the outside of the electrolyte tube and the inside of the Inconel tube with the ceramic cement followed by carefully inserting the electrolyte tube into the Inconel tube. This technique produced a nonuniform seal zone. As a result several other techniques for making the seal were experimentally evaluated using a transparent glass tube to simulate the Inconel tube and thereby permitting observation of the uniformity and density of the ceramic cement at the seal interface. A technique was developed which produced a high density, very uniform ceramic cement seal. This technique involved vibrating the ceramic cement into the seal zone. The forces set up during vibration altered the viscosity of the ceramic cement and allowed it to easily flow into the seal zone. A tube cell assembled using the vibration seal technique produced O_2 with less than 0.2% CO_2 . This bettered the program's O_2 purity goal of less than 0.5% CO_2 -in- O_2 . This test data is discussed in the Program Testing section of this report. Additional details on the tube cell assembly technique can be found in the Electrolyzer Tube Cell Assembly Procedure.

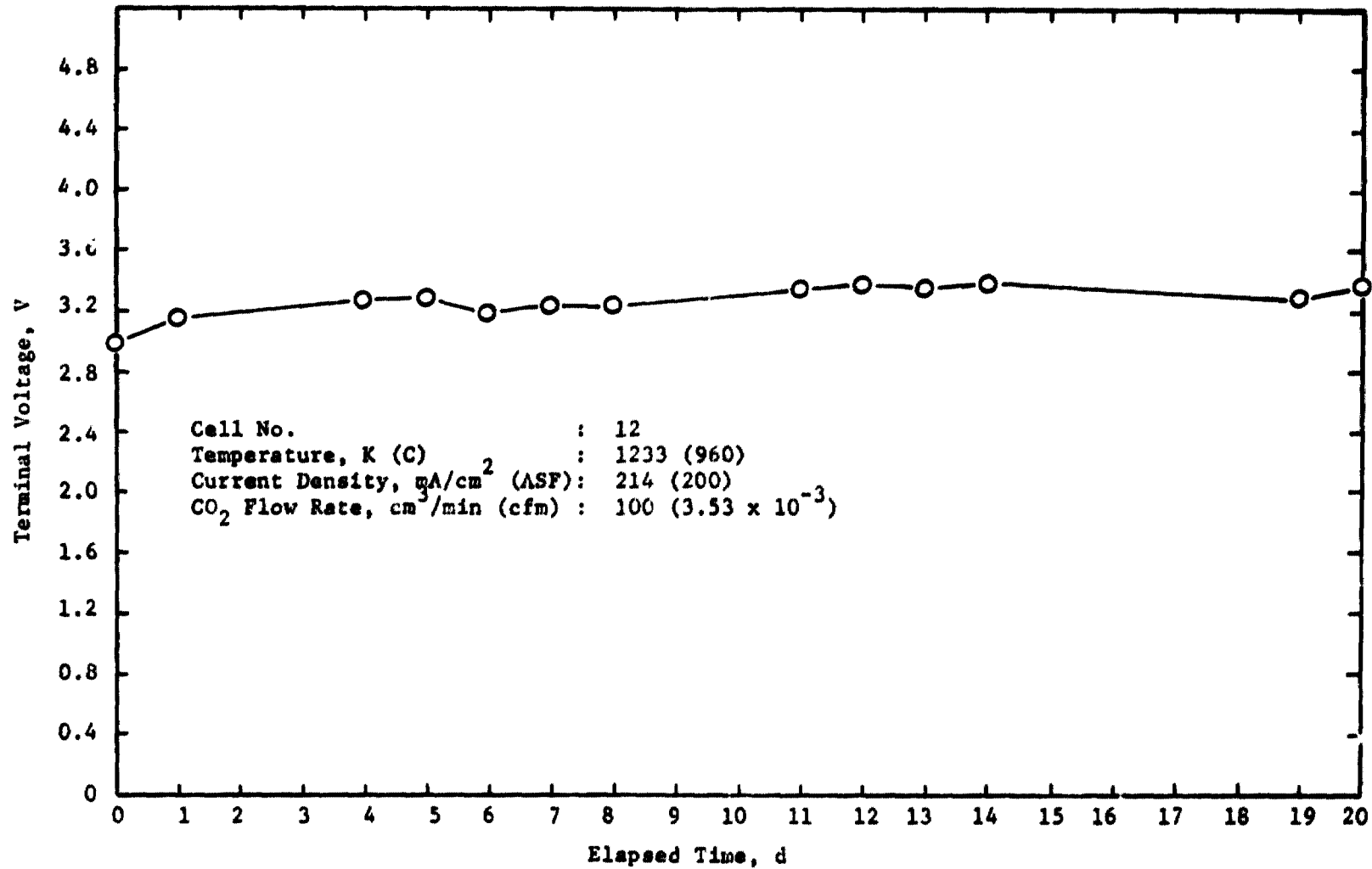


FIGURE 21 ENDURANCE TEST VOLTAGE VERSUS TIME, CELL NO. 12

TABLE 4 CELL NO. 12 ENDURANCE TEST DATA

Cell No. 12
CO₂ Flow = 100 cm³/min (3.5 x 10⁻³ cfm)
Temperature = 1233 K (960 C)
Current Density = 214 mA/cm² (200 ASF)

<u>Date</u>	<u>Day</u>	<u>Terminal Voltage</u>	<u>% CO₂-in-O₂</u>
12/8/77	0	2.97	0.151%
12/9/77	1	3.15	0.121%
12/10/77	2	N.T. (a)	-
12/11/77	3	N.T.	-
12/12/77	4	3.27	0.135%
12/13/77	5	3.29	-
12/14/77	6	3.18	0.141%
12/15/77	7	3.24	-
12/16/77	8	3.25	-
12/17/77	9	N.T.	-
12/18/77	10	N.T.	-
12/19/77	11	3.36	0.140%
12/20/77	12	3.36	-
12/21/77	13	3.36	-
12/22/77	14	3.39	0.153%
12/23/77	15	N.T.	-
12/24/77	16	N.T.	-
12/25/77	17	N.T.	-
12/26/77	18	N.T.	-
12/27/77	19	3.30	0.146%
12/28/77	20	3.37	-

(a) N.T. = Data point not taken.

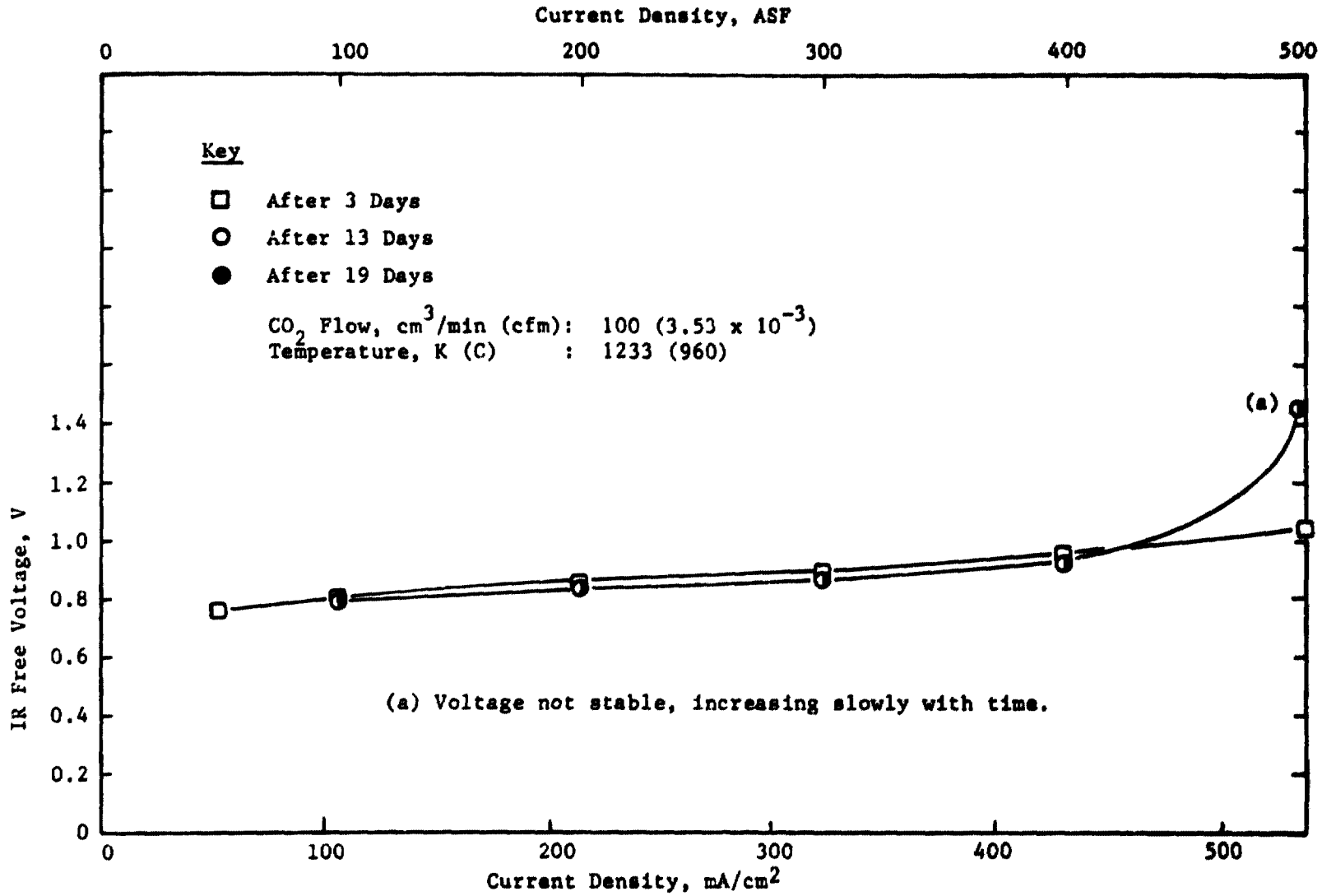


FIGURE 22 CURRENT DENSITY SPANS DURING ENDURANCE TEST, CELL NO. 12

Commercial Electroding Technique

A commercial electrode application technique was evaluated during the program. Early in the program an electrolyte tube was platinized by the commercial technique (LSI-Z) and evaluated.

The evaluation revealed that tube cells with electrodes applied by the LSI-Z technique performed as well as electrolyzer drums with electrodes applied by NAS2-4843 and NAS2-6412 technique. The Pt electrodes were uniform, consistently met the specification of $25 \pm 3 \text{ mg/cm}^2$ ($5.6 \times 10^{-3} \pm 0.7 \times 10^{-3} \text{ oz/in}^2$) Pt loading, exhibited an excellent bond to the electrolyte tube surfaces, and performed well over an extended length of time (200 days). In addition, the commercial electrodes cost one-fifth as much to apply to the electrolyte tube as compared to the NAS2-4843 and NAS2-6412 electrode application technique. As a result, all of the electrolyzer tube cells used for this program contain electrodes applied by the commercial technique.

Tube Cell Terminal Voltage Improvement Study

An IRAD study was conducted to identify methods for reducing the resistive voltage loss of the electrolyzer tube cell. The study revealed that the power requirements could be reduced significantly by decreasing the wall thickness of the electrolyte tube and by increasing (doubling) the diameter of the current-carrying lead wires. The study also pointed out that changing solid electrolyte material to a material with higher ionic conductivity (scandium oxide (Sc_2O_3) stabilized ZrO_2 versus Y_2O_3 stabilized ZrO_2) produces a less significant decrease in power loss when compared to decreasing the electrolyte thickness and increasing the diameter of the leads.

The relative improvement in electrolyzer tube cell terminal voltage expected for various design modifications is shown in Figure 23. The change to a thinner wall electrolyte tube and increased lead diameter are expected to decrease the electrolyzer tube cell power loss by 60% and offer the most attractive next step for the development of low power consuming electrolyzer tube cells.

CONCLUSIONS

Based on the results of this program, the following conclusions can be made:

1. An electrolyzer tube cell which meets the program's O_2 purity specification (less than 0.5% CO_2 in O_2) was developed and evaluated. The electrolyzer cell design characteristics which led to the improved seal were the development of a high density, slip cast electrolyte tube and a design configuration which employs only two high temperature seals.
2. Electrolyzer tube cells can operate with differential pressures of up to at least 6.9 kPa (1 psid) without catastrophic failure or significant increases in leak rate.

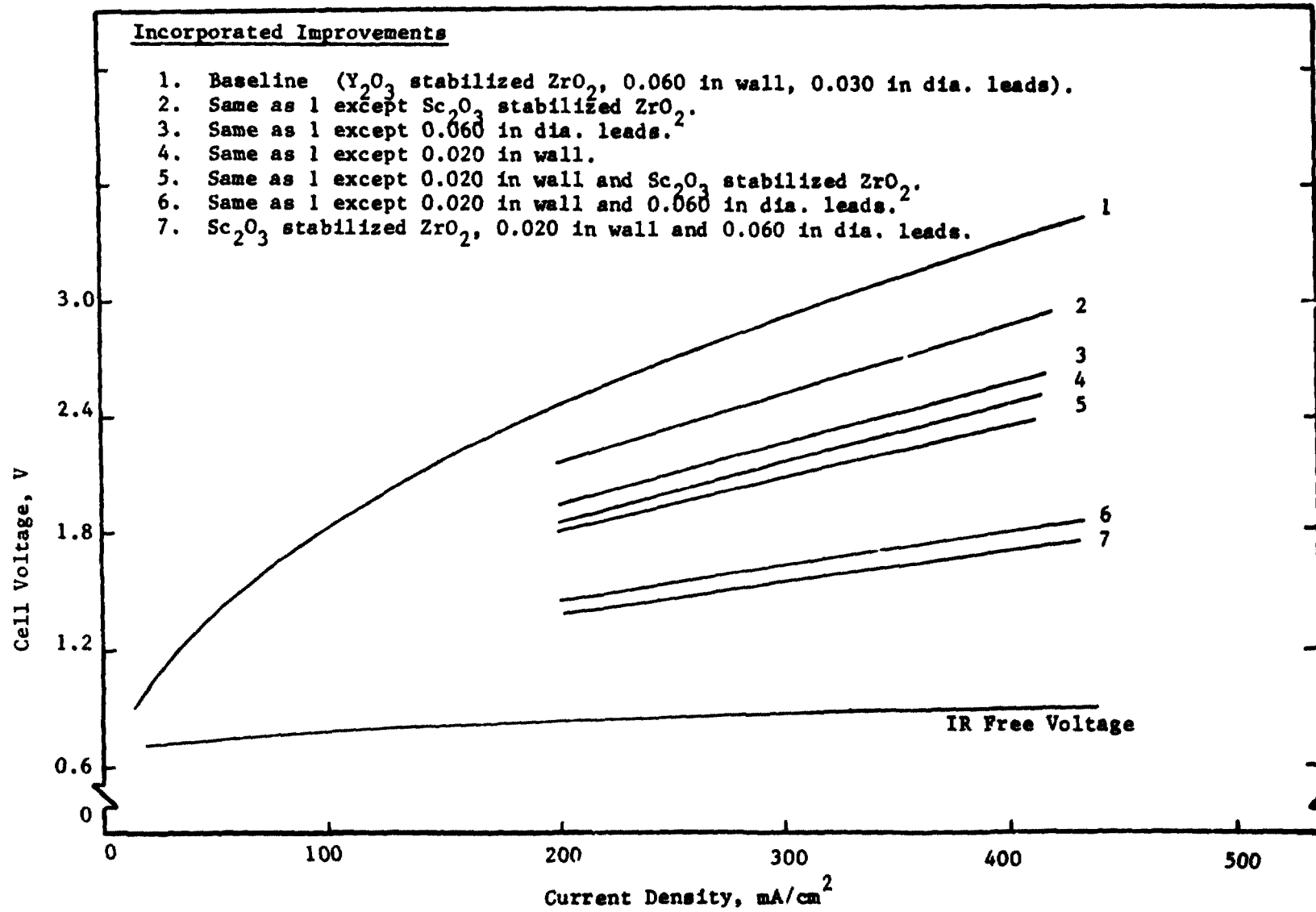


FIGURE 23 PERFORMANCE EXPECTED BY INCORPORATION OF VARIOUS TUBE CELL DESIGN MODIFICATIONS

3. The LSI-Z Pt electrodes applied to the electrolyzer tube cells perform as well as electrodes applied per the techniques developed under Contracts NAS2-2810, NAS2-4843 and NAS2-6412.
4. The minimum electrolyzer tube cell operating temperature that can be used without sacrificing performance is 1203 K (930 C). A slight increase in performance is noted up to 1233 K (960 C) with no significant performance improvement for temperatures greater than 1233 K (960 C). Based on this performance, 1233 K (960 C) was established for the operating temperature of the Y_2O_3 -stabilized ZrO_2 electrolyzer tube cells.
5. The electrolyzer tube cells can operate with any CO_2 /water feed gas ratio.
6. The electrolyzer tube cell can be operated with a CO_2 feed gas flow rate as low as two times the stoichiometric flow rate at all current densities up to at least 538 mA/cm² (500 ASF). This corresponds to a 50% single-pass conversion efficiency.
7. The reduction potential for Y_2O_3 -stabilized ZrO_2 solid electrolyte was experimentally determined to be 1.2 V. This implies that the electrolyzer tube cells can be operated at any current density as long as the IR-free voltage of the cell does not exceed the 1.2 V electrolyte reduction potential.
8. Voltage versus current density data for the tube cell indicate that current densities for both CO_2 and water electrolysis as high as 538 mA/cm² (500 ASF) can be achieved before the electrolyte reduction potential is approached. This implies that extended duration operating current density for a future electrolyzer module may be increased. Future testing is required to determine the actual maximum extended duration current density for the cell.

RECOMMENDATIONS

Based on the successful results of the tube cell development effort, it is recommended that the following activities be carried out in order to expand the technology:

1. Conduct a high current density endurance test to determine the maximum operating current density that an electrolyzer tube cell can operate at for an extended period of time, e.g., 90 days.
2. Conduct an experimental design and fabrication effort to determine the thinnest electrolyte tube that can be fabricated and the largest diameter lead that can be incorporated into the electrolyzer tube cell. Assemble a single cell from the thin electrolyte tube with improved leads and conduct a parametric test program. By minimizing the solid electrolyte thickness and increasing the lead diameter, the cell resistance will be reduced, resulting in lower cell voltages and lower power requirements.

3. Perform an evaluation of the electrolyte tube/Inconel 600 manifold tube joint to determine if the seal length can be reduced. The seal length used for the electrolyzer tube cell development effort described in this report was 10 cm (4 in). It is projected that the seal length can be reduced to less than 2.5 cm (1 in) while still being leak-tight. The objective of decreasing the seal length of the tube cell is to minimize the volume of the one-man electrolyzer module that will be needed in the Solid Electrolyte Oxygen Regeneration System (SX-1).
4. Conduct a test study to determine the maximum anode/cathode differential pressure that the electrolyzer tube cell can withstand without resulting in catastrophic failure or significant increase in leak rate.
5. Based on the work described in Recommendations 1 through 4, design, develop, fabricate, assemble and test an electrolyzer module incorporating tube cells. It is recommended that the module be designed so that it is capable of simultaneously electrolyzing CO₂ and water vapor. This feature is required to eliminate the need for two recycle loops in the SX-1, one for CO₂ and a separate one for water. The elimination of one hot gas recycle loop will decrease system weight, volume and power requirements and will simplify system operation and control.
6. Upon successful completion of the development and evaluation of the electrolyzer module, it is recommended that SX-1 be refurbished and modified to incorporate the electrolyzer module based on tube cells. Upon completion of the refurbishment activities, it is recommended that the SX-1 be subjected to parametric and endurance testing.

REFERENCES

1. "Trade-Off Study and Conceptual Designs of Regenerative Advanced Integrated Life Support Systems (AILSS)," NASA CR-1458, United Aircraft Corporation, Windsor Locks, CT, January, 1970.
2. Shumar, J. W., See, G. G., Schubert, F. H. and Powell, J. D., "Solid Electrolyte Oxygen Regeneration System," Interim Report, NASA CR-137813, Life Systems, Inc. Cleveland, OH, July, 1976.
3. Weissbart, J. and Smart, W. H., "Study of the Electrolyte Dissociation of CO_2 - H_2O Using a Solid Oxide Electrolyte," NASA CR-680, Lockheed Missiles and Space Company, Palo Alto, CA, February, 1967.
4. "Electrolyzer Drum and Module Fabrication and Assembly Procedures," NAS2-7862, ER-190-8-14, Life Systems, Inc., Cleveland, OH, June, 1975.
5. Weppner, W., "Formation of Intermetallic Pt-Zr Compounds Between Pt Electrodes and ZrO_2 -Based Electrolytes, and the Decomposition Voltage of Yttria-Doped ZrO_2 ," J. Electroanal. Chem., 84, (1977), pp 339-350.
6. IBID, p 347.
7. "Electrolyzer Tube Cell Fabrication Procedure," NAS2-7862, ER-190-28, Life Systems, Inc., Cleveland, OH, January, 1978.